JACS
JOURNAL OF THE AMERICAN CHEMICAL SOCIETY

ARTICLE

pubs.acs.org/JACS

# Discrete, Solvent-Free Alkaline-Earth Metal Cations: Metal···Fluorine Interactions and ROP Catalytic Activity

Yann Sarazin,*[,†] Bo Liu,[†] Thierry Roisnel,[†] Laurent Maron,[‡] and Jean-François Carpentier*[,†]

[†]UMR 6226 Sciences Chimiques de Rennes, Université de Rennes 1-CNRS, Campus de Beaulieu, 35042 Rennes Cedex, France
[‡]LPCNO, UMR 5215, Université de Toulouse-CNRS, 135 avenue de Rangueil, 31077 Toulouse, France

Supporting Information

**ABSTRACT:** Efficient protocols for the syntheses of well-defined, solvent-free cations of the large alkaline-earth (Ae) metals (Ca, Sr, Ba) and their smaller Zn and Mg analogues have been designed. The reaction of 2,4-di-*tert*-butyl-6-(morpholinomethyl)phenol ({**LO**$^1$}**H**), 2-{[bis(2-methoxyethyl)amino]methyl}-4,6-di-*tert*-butylphenol ({**LO**$^2$}**H**), 2-[(1,4,7,10-tetraoxa-13-azacyclopentadecan-13-yl)methyl]-4,6-di-*tert*-butylphenol ({**LO**$^3$}**H**), and 2-[(1,4,7,10-tetraoxa-13-azacyclo-pentadecan-13-yl)methyl]-1,1,1,3,3,3-hexafluoropropan-2-ol ({**RO**$^3$}**H**) with $[H(OEt_2)_2]^+[H_2N\{B(C_6F_5)_3\}_2]^-$ readily afforded the doubly acidic pro-ligands $[\{LO^1\}HH]^+[X]^-$ (**1**), $[\{LO^2\}HH]^+[X]^-$ (**2**), $[\{LO^3\}HH]^+[X]^-$ (**3**), and $[\{RO^3\}HH]^+[X]^-$ (**4**) ($[X]^- = [H_2N\{B(C_6F_5)_3\}_2]^-$). The addition of **2** to $Ca[N(SiMe_3)_2]_2(THF)_2$ and $Sr[N(SiMe_3)_2]_2(THF)_2$ yielded $[\{LO^2\}Ca(THF)_{0.5}]^+[X]^-$ (**5**) and $[\{LO^2\}Sr(THF)]^+[X]^-$ (**6**), respectively. Alternatively, **5** could also be prepared upon treatment of $\{LO^2\}CaN(SiMe_3)_2$ (**7**) with $[H(OEt_2)_2]^+[X]^-$. Complexes $[\{LO^3\}M]^+[X]^-$ (M = Zn, **8**; Mg, **9**; Ca, **10**; Sr, **11**; Ba, **12**) and $[\{RO^3\}M]^+[X]^-$ (M = Zn, **13**; Mg, **14**; Ca, **15**; Sr, **16**; Ba, **17**) were synthesized in high yields (70−90%) by reaction of **3** or **4** with the neutral precursors $M[N(SiMe_3)_2]_2(THF)_x$ (M = Zn, Mg, $x = 0$; M = Ca, Sr, Ba, $x = 2$). All compounds were fully characterized by spectroscopic methods, and the solid-state structures of compounds **1**, **3**, **7**, **8**, **13**, **14**, $\{\mathbf{15}\}_4\cdot\mathbf{3CD_2Cl_2}$, $\{\mathbf{16}\}_4\cdot\mathbf{3CD_2Cl_2}$, and $\{\{\mathbf{17}\}_4\cdot\mathbf{EtOH}\}\cdot\mathbf{3CD_2Cl_2}$ were determined by X-ray diffraction crystallography. Whereas the complexes are monomeric in the case of Zn and Mg, they form bimetallic cations in the case of Ca, Sr and Ba; there is no contact between the metal and the weakly coordinating anion. In all metal complexes, the multidentate ligand is $\kappa^6$-coordinated to the metal. Strong intramolecular M···F secondary interactions between the metal and F atoms from the ancillary ligands are observed in the structures of $\{\mathbf{15}\}_4\cdot\mathbf{3CD_2Cl_2}$, $\{\mathbf{16}\}_4\cdot\mathbf{3CD_2Cl_2}$, and $\{\{\mathbf{17}\}_4\cdot\mathbf{EtOH}\}\cdot\mathbf{3CD_2Cl_2}$. VT $^{19}F\{^1H\}$ NMR provided no direct evidence that these interactions are maintained in solution; nevertheless, significant Ae···F energies of stabilization of 25−26 (Ca, Ba) and 40 kcal·mol$^{-1}$ (Sr) were calculated by NBO analysis on DFT-optimized structures. The identity and integrity of the cationic complexes are preserved in solution in the presence of an excess of alcohol (BnOH, $^i$PrOH) or L-lactide (L-LA). Efficient binary catalytic systems for the *immortal* ring-opening polymerization of L-LA (up to 3 000 equiv) are produced upon addition of an excess (5−50 equiv) of external protic nucleophilic agents (BnOH, $^i$PrOH) to **8**−**12** or **13**−**17**. PLLAs with $M_n$ up to 35 000 g·mol$^{-1}$ were produced in a very controlled fashion ($M_w/M_n \approx 1.10-1.20$) and without epimerization. In each series of catalysts, the following order of catalytic activity was established: Mg ≪ Zn < Ca < Sr ≈ Ba; also, Ae complexes supported by the aryloxide ligand are more active than their parents supported by the fluorinated alkoxide ancillary, possibly owing to the presence of Ae···F interactions in the latter case. The rate law $-d[L\text{-}LA]/dt = k_p\cdot[L\text{-}LA]^{1.0}\cdot[\mathbf{16}]^{1.0}\cdot[BnOH]^{1.0}$ was established by NMR kinetic investigations, with the corresponding activation parameters $\Delta H^{\ddagger} = 14.8(5)$ kcal·mol$^{-1}$ and $\Delta S^{\ddagger} = -7.6(2.0)$ cal·K$^{-1}$·mol$^{-1}$. DFT calculations indicated that the observed order of catalytic activity matches an increase of the L-LA coordination energy onto the cationic metal centers with parallel decrease of the positive metal charge.

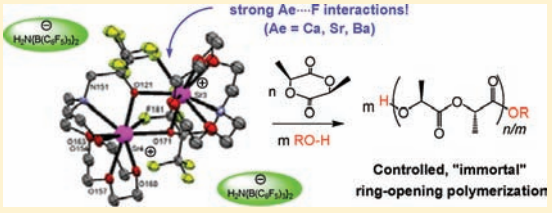


## INTRODUCTION

Biodegradable polyesters such as poly(ε-caprolactone) and poly(lactic acid) (PLA) have attracted widespread interest from industrial and academic research groups and are now widely used in industry.[1] Although they can be obtained by polycondensation reactions, these polymers are best prepared by ring-opening polymerization (ROP) of cyclic esters. Enantiomerically pure L-lactide (L-LA, the cyclic dimer of *S*-lactic acid) is an attractive bioresourced monomer[1a,d] produced on a large scale,[2] and poly(L-LA) (PLLA) exhibits physical and mechanical properties often compared to those of polystyrene.[3] For these reasons, it has become one of the benchmark monomers for catalyst development in this area. Although largely employed in the industry for ROP purposes essentially because of its low cost and robustness,[1b,c,4] tin(II) bis(2-ethylhexanoate) does not afford high activities or good control over the ROP parameters. By contrast, discrete metallic initiators, based mostly on rare earths,[5]

**Received:** March 19, 2011
**Published:** May 05, 2011





dx.doi.org/10.1021/ja2024977 | *J. Am. Chem. Soc.* 2011, 133, 9069–9087

aluminum,[6,7] and zinc,[8] have appeared for the living and (stereo)controlled ROP of cyclic esters, and these (and other) neutral initiators have been highlighted by several reviews.[1e,4,9] Besides, well-defined cationic complexes based on zinc,[10] magnesium,[10b,11] or rare earths[5n,12] have also emerged as potent ROP initiators,[13,14] and the groups of Waymouth and Hedrick have triggered the remarkable development of organic initiators.[15] Another important development in this chemistry is the extension of these living initiating systems into "immortal" systems, upon addition to the metal catalyst of an external protic chain transfer agent or initiator,[5n,r,16] a concept originally pioneered by Inoue for the ROP of epoxides.[17]

ROP initiators based on the large alkaline-earth metals (Ae) calcium, strontium, and barium have so far not enjoyed the popularity of other metal complexes, and only a handful of well-defined neutral heteroleptic Ae ROP catalysts are known.[8h,18,19] This situation reflects the paucity of information available in the literature regarding the synthesis, stability, and reactivity of complexes of these large,[20] extremely electropositive metals. Recurring issues typical of Ca, Sr, and Ba complexes include kinetic lability—with Schlenk-type equilibria in solution often proving highly deleterious—and high basicity of organometallic derivatives.[21] Nevertheless, significant efforts have been accomplished of late in order to tame and exploit the high reactivity of these complexes: strategies aimed at suppressing solution distribution equilibria through the judicious selection of ancillary ligands (such as tris(pyrazolyl)borates,[22] $\beta$-diketiminates,[23] aminotrop(on)iminates[24])[25] or bulky nucleophilic substituents have been devised,[18h,21d,26] while the range of synthetic precursors is growing steadily.[27,28] As a result, single-site Ae-based catalysts have shown astounding ability for a variety of transformations involving $\sigma$-bond metathesis processes.[29]

By analogy with group 4 and rare earth catalysts for olefin polymerization,[30] a better understanding of the reactivity of Ae species and the development of increasingly efficient Ae catalytic systems involves the study of well-defined cationic complexes. Based on a literature survey, it occurred to us that three factors were crucial for the preparation of well-defined $[\{L_nX\}Ae]^+[X]^-$ ion pairs for ROP ($\{L_nX\}^-$ = monoanionic ancillary ligand): (i) the ligand must provide sufficient steric bulk and electron density for the stabilization of these extremely electrophilic species, (ii) weakly coordinating anions $X^-$ yield cations with enhanced Lewis acidity, and (iii) efficient and reliable synthetic protocols devoid of complications due to the presence of Schlenk-type equilibria must be devised. The difficulty of the challenge is real considering the oxophilicity and electropositivity of Mg, Ca, Sr, and Ba, and yet it is pertinent since the increase of Lewis acidity at the metal center should in particular result in higher catalytic efficiency.[31] A first step was achieved in 2001 by Itoh and Kitagawa, who structurally characterized cations of Mg, Ca, and Sr stabilized by a (aza-crown-ether)-aryloxide ligand and external Lewis bases and studied the physicochemical and redox properties of these (as well as that of the Ba derivative) aryloxides and aryloxyl radicals.[32] Inspired by their seminal work, we employed this ligand framework and developed original synthetic protocols to prepare the first solvent-free, well-defined cationic Ae complexes and used the latter as catalysts for the immortal ROP (*i*ROP) of L-LA.[33] This was very shortly followed by the work from Mountford et al., who disclosed cationic calcium tetrahydroborate complexes for the ROP of LA.[34] Finally, Westerhausen et al. have just reported the X-ray structure of the solvent-separated ion pair $[(15\text{-crown-}5)CaCp]^+[(THF)CaCp_3]^-$ (Cp = cyclopentadienyl).[35]

The use of alkoxide ligands for the synthesis of *discrete* Ae complexes is rather limited,[21a,36] evidently because the high $\pi$-donating ability of alkoxides readily results in the formation of polymetallic/polymeric species,[37] especially when large metals are involved. Even more strikingly, no family of well-defined Ae cations supported by alkoxide ligands is known to date: even if the reported structures of diphenylmethanide···(18-crown-6)Ae-enolate ion pairs (Ae = Sr, Ba) are of great interest, the mechanism of their formation was not clearly elucidated.[38] Our previous experience with the use of fluoroalcohols[39] as ligand platforms for the stabilization of oxophilic species prompted us to embark on the synthesis of Ae cations of the type $[\{RO\}Ae]^+[X]^-$ species, where $\{RO\}^-$ is a fluorinated polydentate alkoxide ligand and $X^-$ is a weakly coordinating anion. Indeed, highly fluorinated tertiary alkoxide ligands with bulky, electron-withdrawing $CF_3$ groups in the α position to the alkoxide are weaker $\pi$-donor than conventional alkoxides; they are in many ways similar to the very versatile aryloxide ligands and have allowed the synthesis of several original Ti, Zr, Zn, Al, and Y complexes.[39]

In the present contribution, we describe the preparation of discrete, solvent-free $[\{L_nX\}Ae]^+[H_2N\{B(C_6F_5)_3\}_2]^-$ cationic complexes of Ca, Sr, and Ba and of their lighter congeners Zn and Mg. We show that amino-ether fluoroalkoxide ancillary ligands featuring high denticity enable the synthesis of solvent-free complexes. Strong intramolecular Ae···F secondary interactions between the metal center and F atoms from the ancillary ligands have been observed in the solid state. The synthesis of cationic complexes based on related amino-ether aryloxide ligands is also presented.[33] The catalytic activity of these two classes of complexes in the *i*ROP of L-LA is unveiled, and detailed kinetic and theoretical studies that provide insight into the polymerization mechanisms are also discussed.

## RESULTS AND DISCUSSION

**Syntheses and Characterization.** The syntheses of discrete, solvent-free ion pairs $[\{L_nX\}M]^+[H_2N\{B(C_6F_5)_3\}_2]^-$ (M = Zn, Mg, Ca, Sr, Ba) were initially targeted. The choice of the perfluorinated weakly coordinating anion (WCA) $H_2N\{B(C_6F_5)_3\}_2^-$ developed by Bochmann and co-workers[40] was motivated by two factors. First, it displays crystallization properties better than those of, for instance, the traditional $B(C_6F_5)_4^-$. Whereas the latter can be considered spherical and often leads to the formation of oily or amorphous materials, $H_2N\{B(C_6F_5)_3\}_2^-$ possesses a dipole moment that induces an orientation toward the cation and facilitates crystallization processes. Second, $H_2N\{B(C_6F_5)_3\}_2^-$ is very robust (due to a pattern of internal H···F stabilizing interactions), and the negative charge is delocalized over an extremely large volume (ca. 538 Å$^3$);[41] as a result, the catalytic performances with this anion are at least equivalent to those displayed by smaller fluorinated WCAs.[40,42]

The pro-ligands 2,4-di-*tert*-butyl-6-(morpholinomethyl)phenol ($\{\mathbf{LO^1}\}\mathbf{H}$), 2-{[bis(2-methoxyethyl)amino]methyl}-4,6-di-*tert*-butylphenol ($\{\mathbf{LO^2}\}\mathbf{H}$), 2-[(1,4,7,10-tetraoxa-13-azacyclopentadecan-13-yl)methyl]-4,6-di-*tert*-butylphenol ($\{\mathbf{LO^3}\}\mathbf{H}$), and 2-[(1,4,7,10-tetraoxa-13-azacyclopentadecan-13-yl)methyl]-1,1,1,3,3,3-hexafluoropropan-2-ol ($\{\mathbf{RO^3}\}\mathbf{H}$), were selected as potential ligand platforms of varying denticity to yield stable cationic complexes free of external bases (Figure 1). The new fluorinated

amino-alcohol $\{\mathbf{RO^3}\}\mathbf{H}$ was prepared by slow addition of 3,3,3-trifluoro-2-(trifluoromethyl)-1,2-propenoxide to 1-aza-15-crown-5 in $Et_2O$; it was obtained as a colorless oil, which solidifies by storage at +4 °C. In the $^{19}F\{^1H\}$ NMR spectrum of $\{\mathbf{RO^3}\}\mathbf{H}$, only one singlet is observed at $\delta$ −77.4 ppm, indicating the equivalence of all fluorine atoms. The amino-ether-phenol pro-ligands were prepared as described in the literature.[8n,32,43]

The new compounds $[\{LO^1\}HH]^+[H_2N\{B(C_6F_5)_3\}_2]^-$ (**1**), $[\{LO^2\}HH]^+[H_2N\{B(C_6F_5)_3\}_2]^-$ (**2**), $[\{LO^3\}HH]^+[H_2N\{B(C_6F_5)_3\}_2]^-$ (**3**),[33] and $[\{RO^3\}HH]^+[H_2N\{B(C_6F_5)_3\}_2]^-$ (**4**) were prepared in high yields (≥80%) by treatment of the corresponding pro-ligands with $[H(OEt_2)_2]^+[H_2N\{B(C_6F_5)_3\}_2]^-$ in $Et_2O$ (Scheme 1). Compared to the starting materials, the doubly protonated pro-ligands **1**−**4** can be regarded as diacids where the second acidic proton is systematically located on the nitrogen atom of the amino-ether moiety. The four compounds are fully soluble in $Et_2O$ and chlorinated solvents and sparingly so in aromatic hydrocarbons. The $^1H$ NMR spectra of **1**−**4** in $CD_2Cl_2$ differ significantly from those of their precursors and indicate a decrease in the fluxional behavior of the amino-ether fragment. In all cases, the identity of the $H_2N\{B(C_6F_5)_3\}_2^-$ WCA was confirmed by $^{11}B$ NMR ($\delta$ −8.4 ppm) and by $^{19}F\{^1H\}$ NMR, which show the presence of the diagnostic signals at ca. $\delta$ −133.4, −160.6, and −166.1 ppm; the $^{19}F\{^1H\}$ NMR spectrum of **4** displays an additional resonance (singlet) at $\delta$ −77.5 ppm for both $CF_3$ groups. X-ray quality crystals of **1** and **3**·$CH_2Cl_2$ were grown by recrystallization from $CH_2Cl_2$/pentane mixtures at room temperature; their structures were solved, and the position of the acidic proton was unambiguously located.

Disappointingly, the stoichiometric reaction of **1** with $\{Mg[N(SiMe_3)_2]_2\}_2$ or $Ca[N(SiMe_3)_2]_2(THF)_2$ in $Et_2O$ did not allow the isolation of the desired cationic complexes but instead led to the formation of an intractable mixture from which no compound could be clearly identified (Scheme 2). In THF, $[Mg(THF)_4]^{2+}[H_2N\{B(C_6F_5)_3\}_2^-]_2$ was cleanly obtained, and the presence of the phenolate ligand could not be detected by $^1H$ NMR. Clearly, the ligand $\{LO^1\}^-$ does not provide sufficient steric bulk and/or electronic density to stabilize the targeted $[\{LO^1\}M]^+$ cationic species. Attempts with larger metals (Sr, Ba) were therefore not carried out. By contrast, treatment in $Et_2O$ of $Ca[N(SiMe_3)_2]_2(THF)_2$ or $Sr[N(SiMe_3)_2]_2(THF)_2$ with a stoichiometric amount of **2** yielded the stable, well-defined solvent-separated ion pairs $[\{LO^2\}Ca(THF)_{0.5}]^+[H_2N\{B(C_6F_5)_3\}_2]^-$ (**5**) and $[\{LO^2\}Sr(THF)]^+[H_2N\{B(C_6F_5)_3\}_2]^-$ (**6**) (Scheme 2). In each case, it proved impossible to remove THF under vacuum,

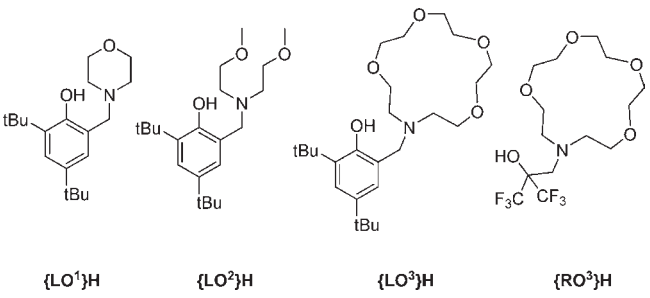


**Figure 1.** Pro-ligands employed in this study.

**Scheme 1. Synthesis of the Doubly Protonated Pro-ligands 1−4**

| | | | |
|---|---|---|---|
| $\{LO^1\}H$ | | $[\{LO^1\}HH]^+[H_2N\{B(C_6F_5)_3\}_2]^-$ | **1** |
| $\{LO^2\}H$ | $[H(OEt_2)_2]^+[H_2N\{B(C_6F_5)_3\}_2]^-$ | $[\{LO^2\}HH]^+[H_2N\{B(C_6F_5)_3\}_2]^-$ | **2** |
| $\{LO^3\}H$ | $Et_2O$ | $[\{LO^3\}HH]^+[H_2N\{B(C_6F_5)_3\}_2]^-$ | **3** |
| $\{RO^3\}H$ | | $[\{RO^3\}HH]^+[H_2N\{B(C_6F_5)_3\}_2]^-$ | **4** |

**Scheme 2. Synthesis of Well-Defined Ae Cationic Complexes**

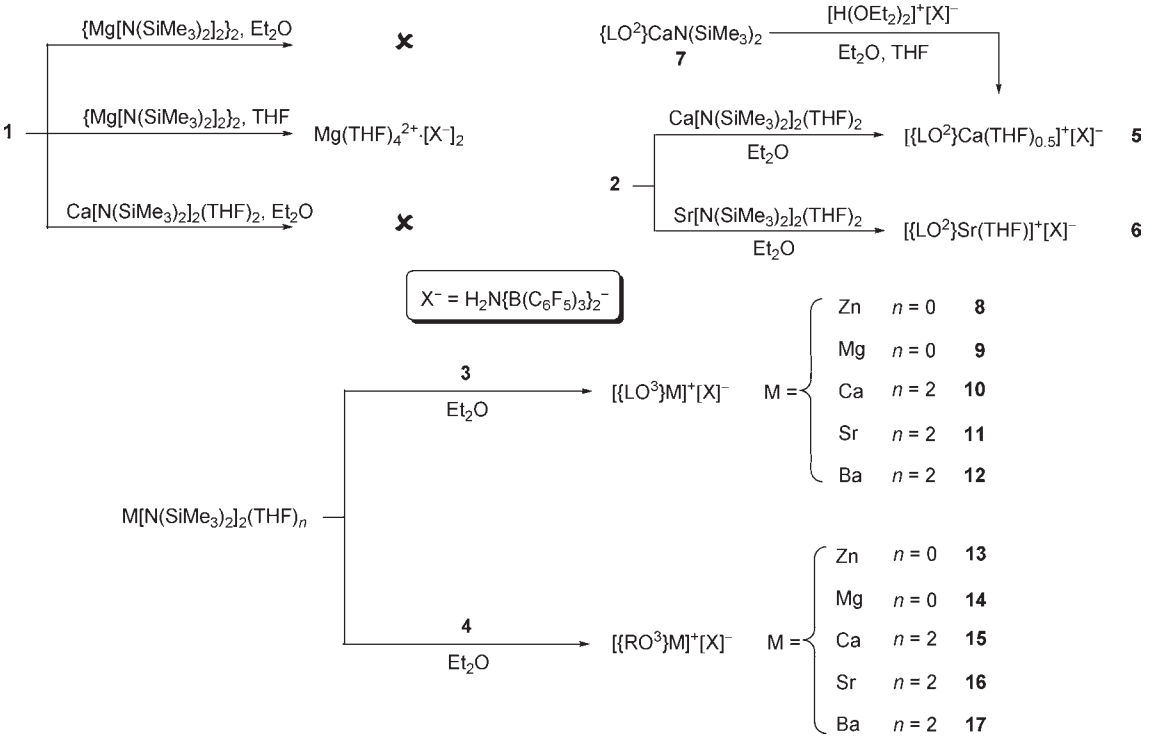



dx.doi.org/10.1021/ja2024977 |J. Am. Chem. Soc. 2011, 133, 9069–9087

even upon gentle heating. This demonstrated that although more stabilizing than $\{LO^1\}^-$, the ligand $\{LO^2\}^-$ is still not sufficiently electron-rich to warrant the formation of solvent-free Ae cations. Importantly, the Ca derivative **5** was also independently synthesized in $Et_2O$ from the neutral heteroleptic complex $\{LO^2\}CaN(SiMe_3)_2$ (**7**, prepared by the 1:1 reaction of $\{LO^2\}H$ and $Ca[N(SiMe_3)_2\text{-}(THF)_2$ in pentane) upon treatment with $[H(OEt_2)_2]^+[H_2N\{B(C_6F_5)_3\}_2]^-$ in the presence of THF (Scheme 2), thus confirming the presence of only half a THF molecule per metal center. This last reaction also indicated that well-defined $[\{L_nX\}M]^+[H_2N\{B(C_6F_5)_3\}_2]^-$ ion pairs (M = Zn, Mg, Ca, Sr, Ba) can in principle be prepared following an alternative procedure, that is, by protonolysis of their heteroleptic precursors $\{L_nX\}MX$ (X = alkyl, amide) with $[H(OEt_2)_2]^+[H_2N\{B(C_6F_5)_3\}_2]^-$. This was particularly exemplified in the case of $\{LO^3\}^-$,[33] but the mandatory preparation of the heteroleptic $\{L_nX\}MX$ compound in this case constitutes a limitation to the method: indeed, owing to detrimental Schlenk-type equilibria, the synthesis of stable heteroleptic species can prove a difficult or even insurmountable task, especially as the size of the metal increases.[44] Complexes **5** and **6** are fully soluble in $CH_2Cl_2$, $Et_2O$, and THF, poorly so in toluene, and insoluble in aliphatic hydrocarbons. They were authenticated by 1D and 2D NMR spectroscopy, and their identity was confirmed by elemental analysis.

Gratifyingly, the solvent-free ion pairs $[\{LO^3\}M]^+[H_2N\text{-}\{B(C_6F_5)_3\}_2]^-$ (M = Zn, **8**; Mg, **9**; Ca, **10**; Sr, **11**; Ba, **12**) and $[\{RO^3\}M]^+[H_2N\{B(C_6F_5)_3\}_2]^-$ (M = Zn, **13**; Mg, **14**; Ca, **15**; Sr, **16**; Ba, **17**) were eventually generated in a one-step protocol by double protonolysis in $Et_2O$ of the suitable homoleptic precursors using the pro-ligands of highest denticity **3** and **4** (Scheme 2). Notably, compounds **8**−**12** can also be obtained by protonolysis of the heteroleptic precursors with $[H(OEt_2)_2]^+[H_2N\{B(C_6F_5)_3\}_2]^-$,[33] but again this first requires the syntheses of $\{LO^3\}MX$ (M = Zn, Mg; X = $N(SiMe_3)_2$, $N(SiMe_2H)_2$, alkyl) or $\{LO^3\}AeN(SiMe_2H)_2$ (Ae = Ca, Sr, Ca),[18h] and the more direct and efficient use of **3** and **4** constitutes the method of choice. Compounds **8**−**12** supported by the aryloxide ligand $\{LO^3\}^-$ are extremely soluble in $Et_2O$, THF, and chlorinated solvents, but hardly so in hydrocarbons. On the other hand, complexes **13**−**16** bearing the fluoroalkoxide $\{RO^3\}^-$ have limited solubilities, even in $CH_2Cl_2$ and $Et_2O$. In fact, they were isolated by precipitation from the reaction mixture ($Et_2O$) during the course of their synthesis. Intriguingly, the barium derivative **17** stands out in the latter family, as it displays the same solubility properties as **8**−**12**. X-ray quality crystals of **8** and $\{\{\mathbf{17}\}_4\cdot\mathbf{EtOH}\}\cdot\mathbf{3CH_2Cl_2}$ were grown by recrystallization from $CH_2Cl_2$/pentane mixture (the presence of EtOH in the latter structure was obviously the outcome of the presence of this stabilizer in $CH_2Cl_2$), while single crystals of **13**, **14**, $\{\mathbf{15}\}_4\cdot\mathbf{3CD_2Cl_2}$, and $\{\mathbf{16}\}_4\cdot\mathbf{3CD_2Cl_2}$ were obtained from concentrated solutions in the deuterated NMR solvent. To our knowledge, **13**−**17** represent the first case of a family of solvent-free, well-defined cationic complexes of the alkaline-earth metals (and zinc) supported by an alkoxide ligand.

All complexes were fully characterized by NMR spectroscopy in $CD_2Cl_2$, and their composition was further substantiated by elemental analysis;[45] in particular, the presence of $Et_2O$ or THF could not be detected. The $^1H$ NMR spectra of **13**−**17** are characterized by numerous overlapping multiplets corresponding to the various methylene units of the aza-15-crown-5 fragment, and generally only the resonances of the methylene groups in the α position to the nitrogen atom in the cation and that of the $NH_2$ bridge (ca. $\delta$ 5.70 ppm) in the WCA could be unambiguously assigned. Diagnostic resonances in the $^{13}C\{^1H\}$ NMR spectra of **13**−**17** include a quartet at low field (ca. $\delta$ 125 ppm, $^1J_{CF}$ = 290−292 Hz) corresponding to the $CF_3$ moieties and another deshielded multiplet of weaker intensity (identifiable as an heptuplet in the cases of **13** and **17**, $^2J_{CF}$ = 26−27 Hz) at ca. $\delta$ 79 ± 2 ppm, assigned to the quaternary carbon bearing the $CF_3$ groups. The $^{11}B$ ($\delta$ −8.4 ppm) and $^{19}F\{^1H\}$ NMR spectra (resonances at $\delta$ −133.4, −160.6, and −166.1 ppm, $^3J_{FF}$ = 18.9 Hz) allow the identification of the $H_2N\{B(C_6F_5)_3\}_2^-$ counterion. Besides, all of the $^{19}F\{^1H\}$-NMR spectra for **13**−**17** also exhibit a singlet attributed to the $CF_3$ groups at $\delta$ −79 ± 1 ppm, i.e., at chemical shifts comparable to those found for $\{RO^3\}H$ and **4**; all fluorine atoms in the ancillary ligand are evidently magnetically equivalent at room temperature. In the case of the large Ca, Sr, and Ba, the complexes in **15**−**17** are found as pairs of bridged bimetallic dications in the solid state (vide infra), with no Ae···F contacts with the WCA. On the other hand, these dications are characterized by the presence of stabilizing internal Ae···F secondary interactions between the metal centers and F atoms from the $\{RO^3\}^-$ ancillaries. The $^{19}F\{^1H\}$ NMR spectra of **15**−**17** recorded at room temperature provided no evidence that the dimeric structure of the complexes is retained in solution. Attempts to observe decoalescence between the signals of free and interacting $CF_3$ groups by VT $^{19}F\{^1H\}$ NMR were thwarted by the poor solubilities of **15** and **16** in $CD_2Cl_2$, $C_6D_5Cl$, or mixtures of toluene-$d_8$ and $o$-$C_6F_4H_2$. In the case of **17** (in $CD_2Cl_2$), distinct broadening but no splitting of the signal at −78.0 ppm was observed by lowering the temperature to −90 °C; this indicates free rotation of the $CF_3$ substituents in solution and suggests that either Ba···F interactions in **17** are not persistent in solution or these interactions are still very fluxional at this low temperature.

The isolation of single crystals of $\{\{\mathbf{17}\}_4\cdot\mathbf{EtOH}\}\cdot\mathbf{3CH_2Cl_2}$ provided evidence that these cationic species were resistant toward the presence of protic sources (alcohols, amines) typically used as initiator/chain transfer agents in *i*ROP. This was further substantiated by several experiments. To assess the robustness of **16**, our catalyst of choice for *i*ROP reactions (vide infra), in the presence of BnOH and L-LA (i.e., the other components in a standard *i*ROP reaction), **16** was reacted with 10 equiv of BnOH in $CH_2Cl_2$ for 3 h at room temperature. Removal of the volatiles and thorough washing with pentane gave unmodified **16** quantitatively; no trace of BnOH or sign of decomposition was detected. This was confirmed by NMR spectroscopy, as the $^1H$ NMR spectrum of **16** and 10 equiv of BnOH in $CD_2Cl_2$ was simply the superimposition of the independent NMR spectra of these two species in $CD_2Cl_2$. Besides, the $^1H$ NMR spectra of **16** and 10 equiv of BnOH in toluene-$d_8$ at 100 °C showed neither sign of reaction nor decomposition of the ion pair. Finally, the stoichiometric reaction of **16** and L-LA in $CH_2Cl_2$ led only to the recovery of unmodified **16** after workup (confirmed by NMR reaction in $CD_2Cl_2$); in fact, **16** recrystallized readily from the reaction mixture in the presence of L-LA at room temperature.

**Crystallographic Studies.** The solid-state structures of the precursors **1**, $\mathbf{3\cdot CH_2Cl_2}$, the neutral heteroleptic complex **7**, and the zinc cationic complexes **8** and **13** have all been determined and are available in the Supporting Information.

The solid-state structures of the Zn and Mg compounds bearing the fluorinated ligand $\{RO^3\}^-$ **13** and **14** were determined.

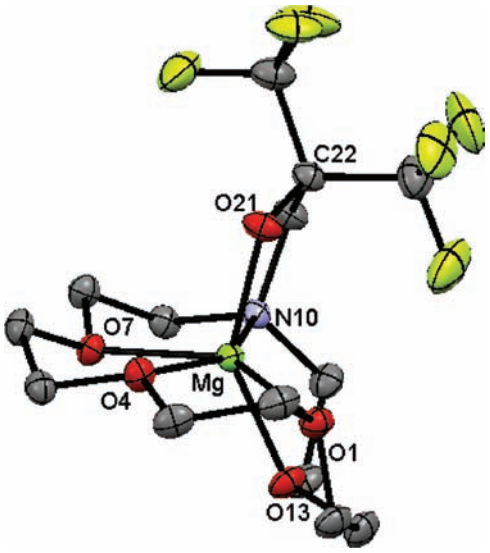


**Figure 2.** ORTEP representation of the cationic fragment $\{RO^3\}Mg^+$ in **14**. Ellipsoids are drawn at the 50% probability level. The counterion $H_2N\{B(C_6F_5)_3\}_2^-$ and hydrogen atoms are omitted for clarity. Selected bond distances [Å] and angles [deg]: Mg−N10 = 2.274(1), Mg−O1 = 2.179(1), Mg−O4 = 2.114(1), Mg−O7 = 2.113(1), M−O13 = 2.135(1), Mg−O21 = 1.913(1); C22−O21−Mg = 121.1(1).

The two compounds are isostructural, and only the structure of the Mg derivative is discussed here (Figure 2). The structure of the counterion $H_2N\{B(C_6F_5)_3\}_2^-$ in **14** (as well as in all other ion pairs that have been characterized by X-ray diffraction crystallography in this work) exhibits the usual pattern of stabilizing H···F interactions; besides, in **14** as in all the remaining cationic complexes, there is no contact between the cation and the WCA.[40a] The cation is monometallic and the metal center is supported only by the ligand coordinated in a $\kappa^6$ fashion. The environment around the metal is best regarded as a distorted octahedral, where the two apical positions are occupied by two oxygen atoms, one from the alkoxide (O21) and one from the macrocycle (O13). There is no contact between the metal and surrounding fluorine atoms, either from the ligand itself or from the WCA. The Mg−$O_{macrocycle}$ (in the range 2.114(1)−2.179(1) Å) and Mg−N10 (2.274(1) Å) bond distances are comparable to those found in **9** (2.109(2)−2.222(2) and 2.238(2) Å, respectively).[33] The Mg−O21 distance and C22−O21−Mg angle values of 1.913(1) Å and 121.1(1)°, respectively, suggest an essentially $\sigma$ interaction between Mg and O21 with no $\pi$ contribution. Interestingly, the deviation from planarity in the macrocycle is far less pronounced in **14** than in its aryloxide derivative **9**, thus highlighting the greater flexibility of the $\{RO^3\}^-$ ligand framework in comparison to $\{LO^3\}^-$. This is obviously related to the replacement of the rigid aryloxide ring by a $sp^3$-hybridized alkoxide group.[6f,39]

Recrystallization of the calcium congener **15** in $CD_2Cl_2$ afforded crystals of $\{\mathbf{15}\}_4\cdot\mathbf{3CD_2Cl_2}$. The cationic metals are associated by pairs, thus forming two independent and almost identical bimetallic dications. In each dication (Figure 3), the two metal centers are bridged by the two $O_{alkoxide}$ atoms (O21 and O71). Each Ca atom in a bimetallic dication is 8-coordinated, and besides the two bridging O-atoms, the coordination sphere for each Ca is completed by N,O,O,O,O atoms of the macrocycle and by one fluorine atom from a $CF_3$ group in the ligand carried by the opposite metal; there is no interaction between the metals and the fluorine atoms of the neighboring $H_2N\{B(C_6F_5)_3\}_2^-$ anions. The Ca1−O21−Ca2−O71 bimetallic core is not planar and exhibits a 20.6° angle between the means planes defined by Ca1−O21−O71 and Ca2−O21−O71. The bond lengths from Ca centers to donor atoms in the aza-15-crown-5 macrocycles (Ca−$O_{macrocycle}$ and Ca−$N_{macrocycle}$ 2.431(4)−2.531(4) and 2.607(5)−2.623(5) Å, respectively) are comparable to those already reported for related compounds.[32,33] The distances to the bridging O21 and O71 oxygen atoms (2.336(4)−2.409(4) Å) are substantially shorter than those to the macrocyclic ones but slightly longer than those found for **10** (2.288 and 2.349 Å)[33] or that to the aryloxide O-atom in Itoh's complex $\{LO^3\}Ca(CH_3OH)_2\cdot BPh_4$ (2.315 Å).[32] Metallophilic interactions can be ruled out on account of the long Ca1···Ca2 distance (3.68 Å; $r_{ionic}$(Ca) = 1.26 Å for C.N. = 8).[20] The distances to the internally interacting fluorine atoms (Ca1−F80 = 2.681(4) Å; Ca2−F25 = 2.664(3) Å) are considerably shorter than the sum of the van der Waals radii for Ca (2.00 Å) and F (1.47 Å)[46] and suggest a significant Ca···F secondary interactions (ca. 25 kcal·mol$^{-1}$ according to DFT calculations, vide infra) in the solid state. Such secondary interactions have been suggested as a way to stabilize reactive Ae centers;[21d,47] recent precedents include Sadow's $[\{(HMe_2Si)_3C\}Ca(THF)_2]^+$ $[HB(C_6F_5)_3]^-$ (Ca···F = 2.41−2.44 Å)[27f] and Hill's calcium bis(amide) complex bearing bulky amides with $CF_3$ substituents (Ca···F = 2.47−2.49 Å).[47c] The Ca···F interaction in $\{\mathbf{15}\}_4\cdot\mathbf{3CD_2Cl_2}$ most probably does not result from crystal packing effects, as suggested by the much longer (4.04−4.63 Å) Ca···F distances to the other two noninteracting fluorine atoms on the $CF_3$ group bearing the bounded one; besides, similar Sr···F and Ba···F stabilizing patterns are found in $\{\mathbf{16}\}_4\cdot\mathbf{3CD_2Cl_2}$ and $\{\{\mathbf{17}\}_4\cdot\mathbf{EtOH}\}\cdot\mathbf{3CH_2Cl_2}$. The strength of these interactions is far from negligible (vide infra) but does not involve significant lengthening of the relevant C−F bond (Ca2···F25−C23 = 1.353(6) Å; Ca1···F80−C78 = 1.355(7) Å) in comparison to those with noninteracting F atoms (C23−F24 = 1.320(7), C23−F26 = 1.344(7) Å; C78−F79, 1.315(7) Å; C23−F81, 1.326(7) Å). Attempts to observe decoalescence in VT $^{19}F\{^1H\}$ NMR studies were precluded by the low solubility of **15** in noncoordinating solvents. In comparison to the Mg parent compound **14**, the higher coordination number and the participation of fluorine atoms to the coordination in **15** reflects the increase in both the metal size and the need for electronic density in the calcium-based complex. Notable contrasting geometric features between the two Ca complexes **10** and **15** include different coordination numbers (7 and 8, respectively) and only a moderate deformation of the macrocyclic fragment in **15**, whereas it folded with a 78.2° angle around the metal in the case of the semirigid $\{LO^3\}^-$.[33]

The structural features of $\{\mathbf{16}\}_4\cdot\mathbf{3CD_2Cl_2}$ resemble those of its Ca homologue (Figure 4). In the dimeric complex, the $Sr_2O_2$ core deviates slightly from planarity, forming an angle of 14.2° between the O21−Sr1−O71 and O21−Sr2−O7 mean planes. Each metal is 8-coordinated: in addition to the two bridging oxygen atoms, the coordination sphere around each metallic center includes the five macrocyclic donating heteroatoms and an additional fluorine atom from the ligand carried by the opposite metal. The two metal atoms sit 3.90 Å apart, excluding any interaction with each other. Interestingly, the Sr−$O_{alkoxide}$ distances (in the range 2.446(7)−2.516(7) Å) show substantial variations, which emphasizes a relative asymmetry in the dicationic fragment. They are clearly longer than the Sr−$O_{aryloxide}$

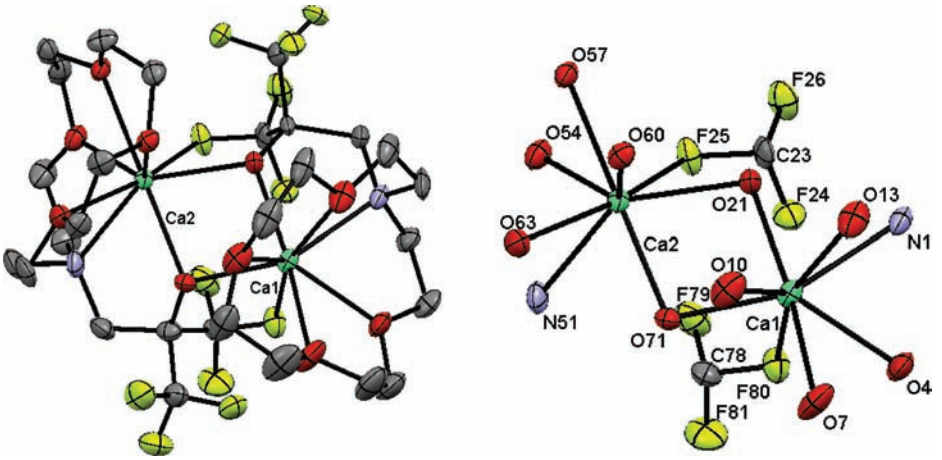


**Figure 3.** ORTEP representation of one of the two independent and equivalent bimetallic cationic fragments $[\{RO^3\}Ca^+]_2$ in $\{\mathbf{15}\}_4\cdot\mathbf{3CD_2Cl_2}$ (left) and corresponding details of the geometry around the metal centers (right). Ellipsoids are drawn at the 50% probability level. The counterions $H_2N\{B(C_6F_5)_3\}_2^-$, noninteracting solvent molecules, and hydrogen atoms are omitted for clarity. Selected bond distances [Å] and angles [deg]: Ca1−N1 = 2.607(5), Ca1−O4 = 2.464(4), Ca1−O7 = 2.531(4), Ca1−O10 = 2.505(4), Ca1−O13 = 2.431(4), Ca1−O21 = 2.336(4), Ca1−O71 = 2.386(4), Ca1−F80 = 2.681(4), Ca2−N51 = 2.623(5), Ca2−O54 = 2.454(4), Ca2−O57 = 2.520(4), Ca2−O60 = 2.522(4), Ca2−O63 = 2.441(4), Ca2−O21 = 2.409(4), Ca2−O71 = 2.351(4), Ca2−F25 = 2.664(3), Ca1−Ca2 = 3.6770(15); Ca1−O21−Ca2 = 101.61(14), Ca2−O71−Ca1 = 101.83(14).

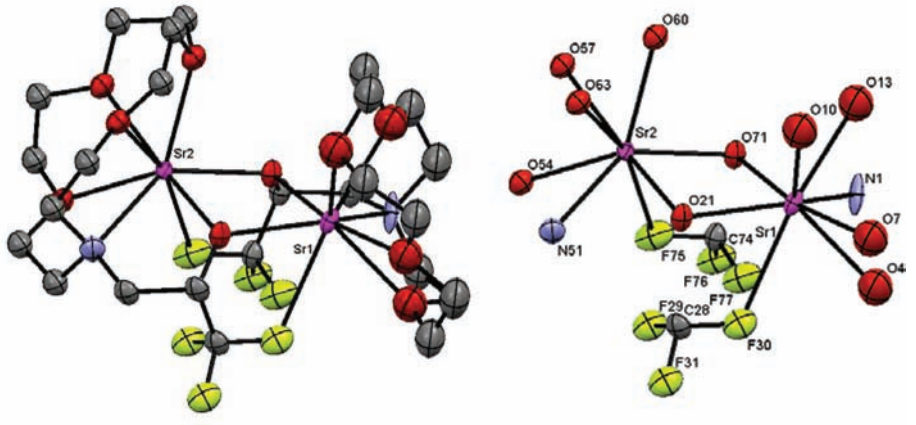


**Figure 4.** ORTEP representation of one of the two independent and equivalent bimetallic cationic fragments $[\{RO^3\}Sr^+]_2$ in $\{\mathbf{16}\}_4\cdot\mathbf{3CD_2Cl_2}$ (left) and details of the geometry around the corresponding metal centers (right). Ellipsoids are drawn at the 50% probability level. The counterions $H_2N\{B(C_6F_5)_3\}_2^-$, solvent molecules, noninteracting $CF_3$ groups, and hydrogen atoms are omitted for clarity. Selected bond distances [Å] and angles [deg]: Sr1−N1 = 2.783(8), Sr1−O4 = 2.596(10), Sr1−O7 = 2.661(10), Sr1−O10 = 2.695(10), Sr1−O13 = 2.531(10), Sr1−O21 = 2.507(7), Sr1−O71 = 2.477(6), Sr1−F30 = 2.859(7), Sr2−N51 = 2.763(9), Sr2−O54 = 2.569(7), Sr2−O57 = 2.620(7), Sr2−O60 = 2.595(7), Sr2−O63 = 2.559(7), Sr2−O21 = 2.446(7), Sr2−O71 = 2.516(6), Sr2−F75 = 2.741(6), Sr1−Sr2 = 3.904; Sr1−O21−Sr2 = 104.0(2), Sr2−O71−Sr1 = 102.9(2), O(21)−Sr(1)−O(71) = 75.2(2), O(21)−Sr(2)−O(71) = 75.6(2).

lengths of 2.36(1) and 2.38(1) Å found by Itoh and Kitagawa for two independent molecules in $[\{L_nO\}Sr(H_2O)]^+[BPh_4]^-$ ($\{L_nO\}^-$ = 2,4-di-*tert*-butyl-6-(1,4,7,10,13-pentaoxa-16-aza-cyclooctadec-16-ylmethyl)aryloxide).[32] The Sr−$O_{macrocycle}$ distances in $\{\mathbf{16}\}_4\cdot\mathbf{3CD_2Cl_2}$ (2.531(1)−2.695(1) and 2.559(7)−2.620(7) Å for Sr1 and Sr2, respectively) are somewhat shorter than those found in the latter compound (2.55−2.77 Å).[32] Moreover, in the $[Ph_2CH]_2[(18\text{-crown-6})Sr(OC_2H_3)]_2$ dimeric enolate complex,[38] the Sr−$O_{enolate}$ (2.395(3)−2.399(3) Å) and Sr−$O_{macrocycle}$ (2.654(4)−2.701(3) Å) bond lengths are also respectively shorter and longer than the corresponding bond distances in $\{\mathbf{16}\}_4\cdot\mathbf{3CD_2Cl_2}$. The interactions between the metal and fluorine atoms appear fairly strong (DFT calculations indicated stabilization of up to ca. 40 kcal·mol$^{-1}$, vide infra). Although not rigorously identical (Sr1−F30 = 2.859(7) Å, Sr2−F75 = 2.741(6) Å), they are both significantly shorter the sum of van der Waals radii for F and Sr.[46] The more intense Sr2−F75 interaction results in a slight elongation of the C74−F75 bond length (1.375(12) Å) in comparison to the C74−F76 and C74−F77 ones (1.309(12) and 1.337(12) Å, respectively). Similar cases of Sr···F secondary interactions were reported for $[\{HC(Pz)_3\}_2Sr]^{2+}[BF_4^-]_2$ (Pz = 3-pyrazolyl; Sr···F−$BF_3$ = 2.450(4)−2.795(4) Å)[48] and in the phenylamide complex $(THF)_6Sr_2[N(H)\text{-}2,6\text{-}F_2C_6H_3]_3I\cdot THF$ (Sr···F = 2.825(4)−2.845(4) Å).[28b]

The asymmetric unit of $\{\{\mathbf{17}\}_4\cdot\mathbf{EtOH}\}\cdot\mathbf{3CH_2Cl_2}$ contains three solvent molecules, two nonequivalent pairs of bridged bimetallic dications and their counterions, one with the expected composition $[\{RO^3\}Ba^+]_2$ and one where the presence of traces


dx.doi.org/10.1021/ja2024977 |*J. Am. Chem. Soc.* 2011, 133, 9069–9087

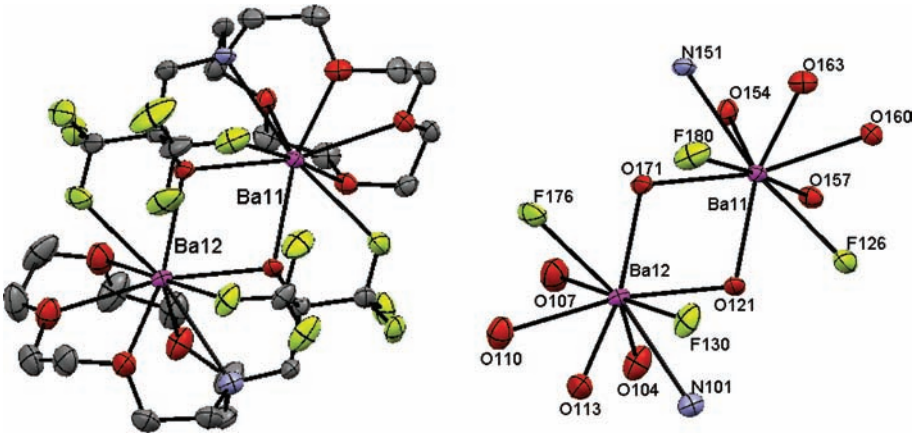


**Figure 5.** ORTEP representation of $[\{RO^3\}Ba^+]_2$ in $\{\{\mathbf{17}\}_4\cdot\mathbf{EtOH}\}\cdot\mathbf{3CH_2Cl_2}$ (left) and details of the geometry around the corresponding metal centers (right). Ellipsoids are drawn at the 50% probability level. Hydrogen atoms are omitted for clarity. Selected bond distances [Å] and angles [deg]: Ba11−N151 = 2.968(3), Ba11−O154 = 2.741(3), Ba11−O157 = 2.805(3), Ba11−O160 = 2.824(3), Ba11−O163 = 2.758(3), Ba11−O121 = 2.615(2), Ba11−O171 = 2.640(3), Ba11−F126 = 2.973(2), Ba11−F180 = 2.971(3), Ba12−N101 = 2.966(3), Ba12−O104 = 2.758(3), Ba12−O107 = 2.823(4), Ba12−O110 = 2.845(3), Ba12−O113 = 2.701(3), Ba12−O121 = 2.655(2), Ba12−O171 = 2.637(3), Ba12−F130 = 2.935(3), Ba12−F176 = 2.992(3), Ba(11)−Ba(12) = 4.2269(3); Ba11−O121−Ba12 = 106.65(8), Ba11−O171−Ba12 = 106.44(8).

of ethanol in the crystallization solvent led to the formation of the adduct $[\{RO^3\}Ba^+]_2\cdot$EtOH. In both cases, there is no contact between the counterions or molecules of $CH_2Cl_2$ and the bimetallic centers. In $[\{RO^3\}Ba^+]_2$ (Figure 5), both metal centers are 9-coordinated by the two bridging $O_{alkoxide}$ atoms, the five heteroatoms from the macrocycle, and *two* fluorine atoms. Note that each of the two $\{RO^3\}^-$ ligands supplies one Ba···F secondary interaction with each metal, that is, the ligand bridges the two Ba atoms not only through $O_{alkoxide}$ but also through its $CF_3$ groups; it is therefore adequately described as a $\mu^2{:}\kappa^7,\kappa^2$-chelate. The $Ba_2O_2$ central core folds by only 7.3° around the O121−O171 axis and is therefore close to planar; however, the bimetallic complex is not symmetrical, and discrepancies in corresponding bonds are observed between the two metals. The long distance between the two Ba atoms (4.227(3) Å) indicates the absence of metallophilic contact. The distances from the Ba atoms to the bridging O atoms (2.615(2)−2.758(3) Å) are only marginally smaller than those to the macrocyclic ones (2.701(3)−2.845(3) Å), possibly a consequence of the extreme size, high electropositivity and low Lewis acidity of barium. They are comparable to those found by Ruhlandt-Senge et al. in a related $[Ph_2CH]_2[(18\text{-crown-6})Ba(OC_2H_3)]_2$ enolate complex.[38] The macrocycle does not show evident signs of distortion, and the N,O,O,O,O core remains almost planar. The Ba···F secondary interactions in $[\{RO^3\}Ba^+]_2$ range from 2.935(3) to 2.992(3) Å; they compare well with those found in the hexafluoroacetylacetonato complex $Ba_2(hfacac)_4\cdot Et_2O$ (2.77−3.09 Å)[49] or the polymeric $[(THF)_2Ba\{N(H)\text{-}2,6\text{-}F_2C_6H_3\}_2]_\infty$ (2.87−2.90 Å)[28b] but are shorter than those reported for $Ba\{amak\}_2$ ({amak}H = $HOC(CF_3)_2CH_2N(CH_2CH_2OMe)_2$, Ba···F = 3.13−3.21 Å).[36d]

The two Ba atoms are not equivalent in $[\{RO^3\}Ba^+]_2\cdot$EtOH (Figure 6). They are bridged by the two $O_{alkoxide}$ atoms, and the central $Ba_2O_2$ is not planar but forms an angle of 22.8° between the mean planes defined by O21−Ba1−O71 and O21−Ba2−O71. Strikingly, a molecule of EtOH is coordinated onto Ba2; its coordination sphere is completed by the N,O,O,O,O atoms of the aza-15-crown-5 cycle and two F atoms (one from its own ligand (F79) and one from the ligand carried by the opposite Ba atom (F25)); Ba2 is therefore formally 10-coordinated. By contrast, Ba1 is only 8-coordinated, as its coordination sphere is devoid of solvent molecule and there is only one interaction with a fluorine atom (F29). The O atom from the solvent molecule (O99) is located at a similar distance from Ba2 (Ba2−O99 = 2.805(3) Å) as the macrocyclic O atoms (Ba2−$O_{macrocycle}$ = 2.832(3)-2.981(2) Å); there is no evidence for a $\pi$-contribution to the Ba2−O99 bond. Coordination of EtOH does not induce significant alterations in the bond lengths around Ba2, as the distances between Ba1 or Ba2 and the O, N and F atoms coordinated respectively on each of them are comparable; besides, all Ba−N, Ba−$O_{alkoxide}$ and Ba−$O_{macrocycle}$ distances in $[\{RO^3\}Ba^+]_2\cdot$EtOH are overall fairly similar to those found in $[\{RO^3\}Ba^+]_2$. The structure of $[\{RO^3\}Ba^+]_2\cdot$EtOH, with coordination onto the metal center of an external protic nucleophilic agent, may be of direct relevance to the study of *i*ROP mechanisms.

**Polymerization of L-LA.** The catalytic activity of the families of complexes **8**−**12** (Table 1) and **13**−**17** (Table 2) toward the immortal ROP of L-LA in the presence of $^i$PrOH or BnOH as an external nucleophilic initiator was assessed. We reasoned that the use of the very weakly coordinating anion $H_2N\{B(C_6F_5)_3\}_2^-$ and the absence of additional Lewis bases on the metal centers should enhance the Lewis acidity of the cations and therefore produce highly active catalysts. Polymerization studies were typically conducted in toluene, with a monomer concentration of 2.0 M, in the temperature range 30−100 °C. Selected data obtained with complexes **8**−**12** and **13**−**17** are collected in Tables 1 and 2. Complexes **5** and **6**, which contain THF, exhibited good activities but limited control under these experimental conditions[50] and were not explored extensively here.

The *i*ROP of L-LA is efficiently promoted by **8** at 100 °C and **10**−**12** at lower temperature (30−60 °C) upon addition of an excess of $^i$PrOH as an external initiator; unexpectedly, the Mg derivative **9** is totally inactive under these experimental conditions. The Zn complex **8** requires elevated temperature (Table 1, entries 1−3) but yields PLLAs with tunable molecular weight in the presence of up to 50 equiv of initiator/chain-transfer agent with good control over the polymerization parameters.[51] Turnover frequencies (TOFs, calculated at <90% conversions) of the


dx.doi.org/10.1021/ja2024977 |*J. Am. Chem. Soc.* 2011, 133, 9069–9087

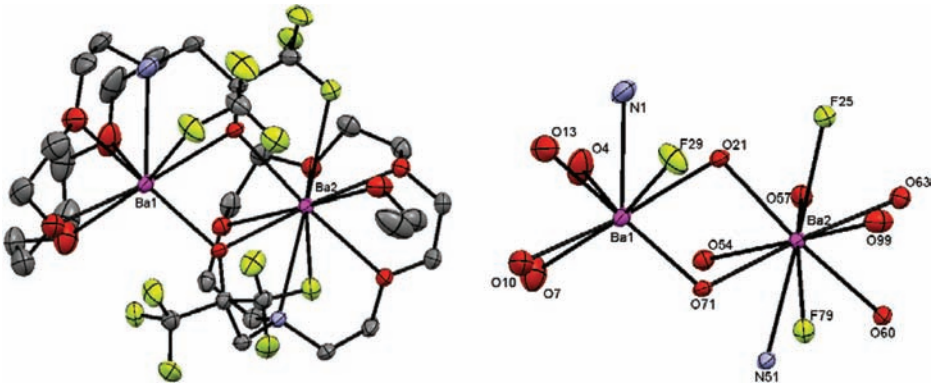


**Figure 6.** ORTEP representation of $[\{RO^3\}Ba^+]_2 \cdot EtOH$ in $\{\{\mathbf{17}\}_4 \cdot \mathbf{EtOH}\} \cdot \mathbf{3CH_2Cl_2}$ (left) and details of the geometry around the corresponding metal centers (right). Ellipsoids are drawn at the 50% probability level. Hydrogen atoms are omitted for clarity. Selected bond distances [Å] and angles [deg]: Ba1−N1 = 2.938(4), Ba1−O4 = 2.769(3), Ba1−O7 = 2.886(4), Ba1−O10 = 2.913(3), Ba1−O13 = 2.810(3), Ba1−O21 = 2.670(2), Ba1−O71 = 2.595(2), Ba1−F29 = 2.960(3), Ba2−N51 = 2.990(3), Ba2−O54 = 2.981(2), Ba2−O57 = 2.844(3), Ba2−O60 = 2.832(2), Ba2−O63 = 2.877(2), Ba2−O21 = 2.662(2), Ba2−O71 = 2.681(2), Ba2−O99 = 2.805(3), Ba2−F25 = 3.084(2), Ba2−F79 = 2.981(2), Ba(1)−Ba(2) = 4.1774(3); Ba1−O21−Ba2 = 103.1(8), Ba1−O71−Ba2 = 104.7(8).

**Table 1. Immortal ROP of L-LA with 8−12/ROH Systems**[a]

| entry | $M^+$ | ROH | [L-LA]/[$M^+$]/[ROH] | $T^{re}$ [°C] | $t$ [h] | yield [%][b] | TOF [mol·(mol·h)$^{-1}$] | $M_{n,theo}$ [g·mol$^{-1}$][c] | $M_{n,SEC}$ [g·mol$^{-1}$][d] | $M_w/M_n$[d] |
|---|---|---|---|---|---|---|---|---|---|---|
| 1 | **8** | $^i$PrOH | 1 000:1:5 | 100 | 16 | 99 | 62 | 28 600 | 31 800[e] | 1.38 |
| 2 | **8** | $^i$PrOH | 1 000:1:10 | 100 | 16 | 99 | 62 | 14 300 | 13 300 | 1.25 |
| 3 | **8** | $^i$PrOH | 1 000:1:50 | 100 | 16 | 97 | 61 | 2 900 | 3 200 | 1.15 |
| 4 | **9** | $^i$PrOH | 1 000:1:10 | 100 | 3 | tr | | | | |
| 5 | **10** | $^i$PrOH | 1 000:1:10 | 60 | 11 | 90 | 82 | 13 000 | 12 900 | 1.07 |
| 6 | **10** | BnOH | 1 000:1:5 | 60 | 8 | 72 | 90 | 20 900 | 17 500 | 1.08 |
| 7 | **10** | BnOH | 1 000:1:10 | 60 | 8 | 72 | 90 | 10 500 | 10 700 | 1.06 |
| 8[f] | **10** | BnOH | 1 000:1:10 | 60 | 7 | 64 | 91 | 9 200 | 8 500 | 1.07 |
| 9 | **10** | BnOH | 1 000:1:10 | 60 | 11 | 83 | 75 | 12 100 | 11 300 | 1.06 |
| 10 | **10** | BnOH | 1 000:1:10 | 60 | 24 | 97 | 40 | 14 000 | 12 800 | 1.10 |
| 11 | **10** | BnOH | 2 000:1:10 | 60 | 24 | 95 | 79 | 27 500 | 19 600[e] | 1.09 |
| 12 | **10** | BnOH | 3 000:1:10 | 60 | 24 | 96 | 120 | 41 600 | 30 000[e] | 1.06 |
| 13 | **10** | BnOH | 1 000:1:20 | 60 | 8 | 78 | 97 | 5 700 | 5 800 | 1.07 |
| 14 | **10** | BnOH | 1 000:1:50 | 60 | 8 | 83 | 104 | 2 500 | 2 400 | 1.12 |
| 15 | **11** | $^i$PrOH | 1 000:1:10 | 30 | 1 | 48 | 480 | 7 000 | 14 000 | 1.20 |
| 16 | **12** | $^i$PrOH | 1 000:1:10 | 100 | 0.05 | 30 | 6 000 | 4 400 | 11 000 | 1.21 |
| 17 | **12** | $^i$PrOH | 1 000:1:10 | 30 | 1 | 34 | 340 | 5 000 | 13 000 | 1.27 |

[a] Polymerizations carried out in toluene with $[\text{L-LA}]_0 = 2.0$ M. [b] Isolated yield after precipitation. [c] Calculated from $M_{n,theo} = [\text{L-LA}]_0/[\text{ROH}]_0 \times \text{yield} \times 144.13 + M_{ROH}$, with $M_{BnOH} = 108$ g·mol$^{-1}$ and $M_{iPrOH} = 60$ g·mol$^{-1}$. [d] Determined by size exclusion chromatography calibrated vs polystyrene standards and corrected by a factor of 0.58 according to literature recommendations.[52] [e] Note that the 0.58 factor applied to the correction of PLLA molecular weights determined vs polystyrene standards is inadequate at high molecular weights; higher factors should be utilized.[53] [f] Run in chloroform.

**8**/$^i$PrOH system were typically in the range 60−65 $\text{mol}_{\text{L-LA}} \cdot (\text{mol}_{Zn} \cdot \text{h})^{-1}$. The agreement between experimental and theoretical molecular weights is satisfactory, and the molecular weight distribution is relatively narrow ($M_w/M_n$ = 1.15−1.38); both observations are consistent with fast and reversible chain transfer between activated (growing) macromolecules and dormant ones.[16] The binary catalytic system **8**/$^i$PrOH thus proceeds in the expected fashion for the ROP of L-LA according to the so-called "activated monomer" mechanism.[16h,33]

The Sr and Ba analogues **11** and **12** constitute highly active binary catalysts in the presence of $^i$PrOH (Table 1, entries 15−17), allowing rapid conversion of the monomer even at 30 °C with TOFs as high as 6 000 $\text{mol}_{\text{L-LA}} \cdot (\text{mol}_{\text{metal}} \cdot \text{h})^{-1}$. Although the molecular weight distributions remain narrow ($M_w/M_n$ = 1.20−1.30) at low conversion (below 50%), the observed molecular weights did not match their calculated values; besides, rapid broadening of the molecular weight distributions was observed at higher conversion (above 70%) because of transesterification side processes (as evidenced by MALDI-TOF MS). Therefore, although very active, these catalytic systems offer limited scope for the *controlled* *i*ROP of cyclic esters.

The Ca derivative **10** offers the best compromise in terms of activity and control and provides a very efficient binary catalyst for well-controlled *i*ROP upon addition of 5−50 equiv of $^i$PrOH (Table 1, entry 5)[33] or BnOH (Table 1, entries 6−14) at 60 °C.[54] Full conversion of up to 3 000 equiv of L-LA was achieved within 24 h, and the control of the polymerization parameters was


dx.doi.org/10.1021/ja2024977 |J. Am. Chem. Soc. 2011, 133, 9069–9087

**Table 2. Immortal ROP of L-LA with 13−17/BnOH Systems**[a]

| entry | $M^+$ | [L-LA]/[$M^+$]/[BnOH] | $T$ [°C] | $t$ [h] | yield[b] [%] | TOF [mol·(mol·h)$^{-1}$] | $M_{n,the}$[c] [g·mol$^{-1}$] | $M_{n,SEC}$[d] [g·mol$^{-1}$] | $M_w/M_n$ |
|---|---|---|---|---|---|---|---|---|---|
| 1 | **13** | 1 000:1:10 | 100 | 3 | 27 | 90 | 4 000 | 4 100 | 1.07 |
| 2 | **14** | 1 000:1:10 | 100 | 3 | tr | | | | |
| 3 | **15** | 1 000:1:10 | 100 | 3 | 47 | 157 | 6 900 | 6 700 | 1.12 |
| 4 | **16** | 1 000:1:10 | 100 | 3 | 74 | 247 | 10 800 | 9 900 | 1.17 |
| 5 | **17** | 1 000:1:10 | 100 | 3 | 50 | 167 | 7 300 | 6 800 | 1.16 |
| 6 | **16** | 1 000:1:10 | 100 | 0.75 | 19 | 253 | 2 800 | 2 800 | 1.09 |
| 7 | **16** | 1 000:1:10 | 100 | 1.5 | 52 | 347 | 7 600 | 7 500 | 1.10 |
| 8 | **16** | 1 000:1:10 | 100 | 2.25 | 61 | 271 | 8 900 | 8 600 | 1.11 |
| 9 | **16** | 1 000:1:10 | 100 | 4.5 | 85 | 189 | 12 400 | 12 100 | 1.42 |
| 10 | **16** | 1 000:1:10 | 100 | 6 | 89 | 148 | 12 900 | 12 100 | 1.30 |
| 11 | **16** | 1 000:1:5 | 100 | 1.5 | 34 | 227 | 9 900 | 9 300 | 1.09 |
| 12 | **16** | 1 000:1:10 | 100 | 1.5 | 52 | 347 | 7 600 | 7 500 | 1.10 |
| 13 | **16** | 1 000:1:20 | 100 | 1.5 | 57 | 380 | 4 200 | 4 100 | 1.10 |
| 14 | **16** | 1 000:1:50 | 100 | 1.5 | 75 | 500 | 2 300 | 2 400 | 1.10 |
| 15 | **16** | 500:1:10 | 100 | 4 | 95[e] | 119 | 7 000 | 7 000 | 1.19 |
| 16 | **16** | (500+)500:1:10 | 1000 | (4+)4 | 91 | 114 | 13 100 | 12 700 | 1.21 |
| 17 | **16** | 2 000:1:5 | 100 | 24 | 85 | 71 | 49 100 | 35 000[f] | 1.41 |

[a] Polymerizations carried out in toluene with $[\text{L-LA}]_0 = 2.0$ M in the presence of BnOH. [b] Isolated yield after precipitation. [c] Calculated from $M_{n,theo} = [\text{L-LA}]_0/[\text{BnOH}]_0 \times \text{yield} \times 144.13 + M_{ROH}$, with $M_{BnOH} = 108.14$ g·mol$^{-1}$. [d] Determined by size exclusion chromatography calibrated vs polystyrene standards and corrected by a factor of 0.58 according to literature recommendations.[52] [e] Conversion determined by NMR. [f] Note that the 0.58 factor applied to the correction of PLLA molecular weights determined vs polystyrene standards is inadequate at high molecular weights; higher factors should be utilized.[53]

excellent ($M_{n,theo} \sim M_{n,SEC}$; $M_w/M_n = 1.06-1.12$). The TOFs were characteristically in the range 80−100 $\text{mol}_{\text{L-LA}}\cdot(\text{mol}_{\text{Ca}}\cdot\text{h})^{-1}$. There is no influence of the contents in BnOH on the catalytic activity in the concentration range examined (5−50 equiv vs **10**); on the other hand, the molecular weights decreased linearly with increasing BnOH contents (compare entries 6, 7, 13, and 14). As anticipated for an *i*ROP mechanism, the nature of the initiator had little influence on the activity (BnOH, 90 $\text{mol}_{\text{L-LA}}\cdot(\text{mol}_{\text{Ca}}\cdot\text{h})^{-1}$, entry 7; $^i$PrOH, 82 $\text{mol}_{\text{L-LA}}\cdot(\text{mol}_{\text{Ca}}\cdot\text{h})^{-1}$, entry 5) and none on the molecular weight features. Moreover, at this temperature, the polymerization proceeded equally fast in $CHCl_3$ (Table 1, entry 8) as in toluene (Table 1, entry 7). No epimerization of the optically active centers was detected by $^1$H NMR. Kinetic studies (reactions performed in Schlenk vessel, see the Supporting Information) indicated a first-order dependence on monomer concentration; at $[\text{L-LA}]_0 = 2.0$ M, $T = 60$ °C and $[\text{L-LA}]_0/[\mathbf{10}]_0/[\text{ROH}]_0 = 1\,000{:}1{:}10$, the apparent rate constants with $^i$PrOH[33] and BnOH were $k_{app}^{^i\text{PrOH},60} = 0.210$ h$^{-1}$ and $k_{app}^{\text{BnOH},60} = 0.170$ h$^{-1}$, respectively. For the binary system **10**/BnOH, $k_{app}^{\text{BnOH},60}$ was determined at various catalyst concentrations ($[\mathbf{10}]_0 = 2.00-20.0$ mM) and fixed L-LA (2.0 M) and BnOH (20 mM) concentrations and spanned from 0.17 h$^{-1}$ ($[\mathbf{10}]_0 = 2.00$ mM) to 2.70 h$^{-1}$ ($[\mathbf{10}]_0 = 20.0$ mM). The corresponding logarithmic plot of monomer conversion versus catalyst concentration gave a non-integer order of 1.20 in catalyst concentration. Such fractional orders have already been reported for Zn[8b] and Y[55] catalysts before and are diagnostic of the formation of aggregated metallic species. The dependence on alcohol concentration was not investigated at this stage. The controlled character of the *i*ROP catalyzed by **10**/BnOH (or $^i$PrOH) was established by NMR spectroscopy performed on low molecular weight PLLA samples and MALDI-TOF mass spectrometry. They confirmed that the nature of the polymer end-groups consisted of the expected $-CH(CH_3)OH$ and $BnO-C(O)-CHCH_3-$ moieties resulting from acyl cleavage by BnOH (or $^i$PrOH); the presence of other termini could not be detected. Two Bernouillian distributions (sometimes of equal intensity) separated by increments of 72 Da were usually observed in the MALDI-TOF mass spectra of the polymers, indicating that transesterification processes occur very rapidly with these systems (vide supra).

Effective binary catalytic systems are also generated upon addition of an excess of BnOH to the fluorinated complexes **13** and **15**−**17** (Table 2, entries 1−5). Incomplete conversion of 1 000 equiv of L-LA was observed at 100 °C with $[\text{L-LA}]_0/[\text{M}^+]_0/[\text{BnOH}]_0 = 1\,000{:}1{:}10$, with the Sr and Ba derivatives being the most active and Zn and Mg the least ones. In particular, we found that the Mg complex **14** is, like previously with **9**, almost entirely inactive under the given experimental conditions (Table 2, entry 2). The reasons for this behavior are unclear at this stage but probably relate to the small size of Mg, its high Lewis acidity, and the high chelating ability of the ligands. General features of the systems **13** and **15**−**17**/BnOH include (i) relatively lower catalytic activity than their aryloxide counterparts **8**−**12**, requiring higher polymerization temperature (100 °C or so) with TOFs in the range 100−500 $\text{mol}_{\text{L-LA}}\cdot(\text{mol}_{\text{metal}}\cdot\text{h})^{-1}$, (ii) very good control over the polymerization, with good agreement between $M_{n,theo}$ and $M_{n,SEC}$ and generally very narrow distributions ($M_w/M_n \sim 1.10-1.20$), and (iii) absence of epimerization of the chiral centers.

The most efficient system **16**/BnOH based on the Sr catalyst was subjected to scrutiny (Table 2, entries 6−17). The catalyst is able to polymerize 2 000 equiv of L-LA and to withstand up to 50 equiv of BnOH without detrimental effect to the catalytic activity or to the control (entries 11−14; reactions times were deliberately limited to maintain incomplete conversion). In fact, the activity increased regularly with alcohol content, suggesting a kinetic dependence on the concentration of initiator. Moreover, at comparable conversion, the molecular

weight decreased linearly with increasing alcohol contents (Table 2, entries 11−14). At fixed $[\text{L-LA}]_0/[\mathbf{16}]_0/[\text{ROH}]_0$ = 1 000:1:10 (Table 2, entries 6−10; $[\text{L-LA}]_0 = 2.0$ M), an increase of conversion with reaction time and a linear increase of molecular weights with conversion were observed. The molecular weight distribution remained very narrow up to ca. 80% conversion, when broadening occurred, most likely as a result of transesterification reactions. The semilogarithmic plot of monomer conversion versus reaction time indicated a first-order dependence on monomer concentration, and the corresponding calculated apparent rate constant was $k_{app}^{100,\text{BnOH}} = 0.376\ \text{h}^{-1}$.[56] A double-feed experiment was carried out to demonstrate the immortal nature of the catalytic system (Table 2, entries 15 and 16): a first batch of 500 equiv of L-LA was polymerized with 4 h. An aliquot was collected for NMR and SEC analyses, and another load of 500 equiv of monomer was added to the reaction medium. Near quantitative conversion of the monomer was achieved after an additional 4 h. The molecular features of the polymers after conversion of 500 and 1 000 equiv of L-LA were identical ($M_w/M_n$ = 1.19 and 1.21, respectively), and the molecular weight increased by the expected value based on monomer conversion. NMR and MALDI-TOF MS analyses showed that the polymers prepared with BnOH/**16** (as well as its derivatives **13**, **15**, and **17**) possessed $-\text{CH}(\text{CH}_3)\text{OH}$ and $\text{BnO}-\text{C(O)}-\text{CH}(\text{CH}_3)-$ termini, as expected for PLLA chains resulting from initial ring opening of L-LA by BnOH followed by further monomer addition to the (macro)alcohols.[16h,33] This was further corroborated by NMR monitoring of the reaction of L-LA and 1.0 equiv of BnOH in the presence of 0.1 equiv of **16**, which showed complete formation of the opened product $\text{BnO}-\text{C(O)}-\text{CH}(\text{CH}_3)-\text{O}-\text{C(O)}-\text{CH}(\text{CH}_3)-\text{OH}$ after 1 h in $CD_2Cl_2$ at room temperature. Besides, the reaction of L-LA, 0.5 equiv of BnOH and 0.05 equiv of **16** in toluene-$d_8$ at 100 °C gave the double insertion product $\text{BnO}-\text{C(O)}-\text{CH}(\text{CH}_3)-[\text{O}-\text{C(O)}-\text{CH}(\text{CH}_3)]_2-\text{O}-\text{C(O)}-\text{CH}(\text{CH}_3)-\text{OH}$ within 10 min.

**Polymerization Kinetics.** The binary catalyst **16**/BnOH was selected for detailed *i*ROP kinetic studies in order to establish the rate law. The choice of the Sr complex **16** was motivated by practical reasons: it is very robust in solution in the presence of L-LA and/or BnOH (vide supra), fairly active over the course of a few hours at 80−100 °C but is almost inactive at room temperature. Kinetic studies were thus performed by NMR spectroscopy at 100 °C in toluene-$d_8$. At fixed monomer and initiator (BnOH) concentrations (2.0 M and 96.67 mM, respectively), the conversion of L-LA with time was monitored by $^1$H NMR spectroscopy at various catalyst concentrations ($[\mathbf{16}]_0$ = 3.26−32.61 mM) until full conversion was observed. First order dependence was observed in each case, and the corresponding apparent rate constants ($k_{app}$ = 0.0003−0.0033 $\text{s}^{-1}$) were extracted from the semilogarithmic plots $\ln([\text{L-LA}]_0/[\text{L-LA}]_t) = k_{app}\cdot t$. No induction period was observed. The plot of $\ln(k_{app})$ versus $\ln([\mathbf{16}]_0)$ was linear, and the gradient of the best-fit line was 1.04$_7$ (Figure 7). Therefore, the kinetic order in catalyst is equal to 1.0 within experimental errors.

The dependence on initiator concentration was also determined. At fixed monomer ($[\text{L-LA}]_0$ = 2.0 M) and catalyst ($[\mathbf{16}]_0$ = 14.67 mM) concentrations, the conversion of monomer with time was monitored at various initiator concentrations ($[\text{BnOH}]_0$ = 29.0−290 mM). Again, the consumption of the monomer followed accurately first-order kinetics, and there was no induction period (Figure 8). Hence the kinetic order in initiator is 1.0, which eventually gives the following rate law:

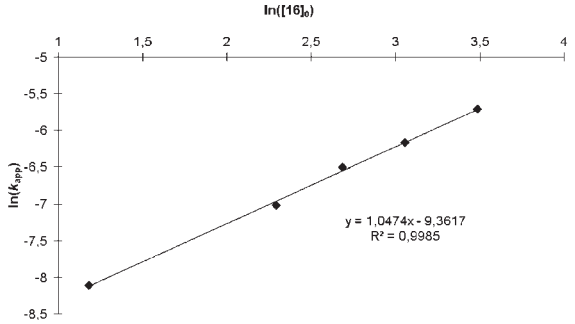


**Figure 7.** Plot of $\ln(k_{app})$ versus $\ln([\mathbf{16}]_0)$ for the polymerization of L-LA promoted by **16**/BnOH at various catalyst concentrations (3.26−32.61 mM) and fixed $[\text{BnOH}]_0$ (96.67 mM) and $[\text{L-LA}]_0$ (2.0 M) concentrations. Polymerizations carried out in toluene-$d_8$ at 100 °C.

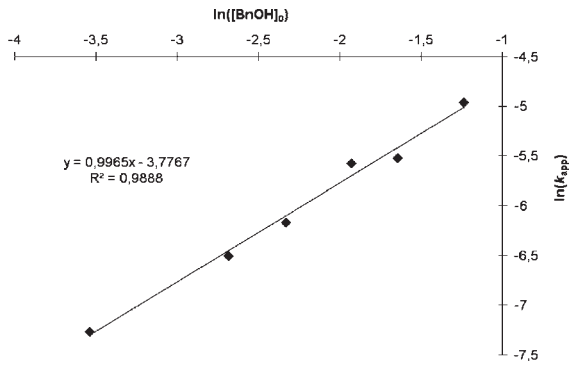


**Figure 8.** Plot of $\ln(k_{app})$ versus $\ln([\text{BnOH}]_0)$ for the polymerization of L-LA promoted by **16**/BnOH at various initiator concentrations (29.0−290 mM) and fixed $[\mathbf{16}]_0$ (14.67 mM) and $[\text{L-LA}]_0$ (2.0 M) concentrations. Polymerizations carried out in toluene-$d_8$ at 100 °C.

$$-\text{d}[\text{L-LA}]/\text{d}t = k_p\cdot[\text{L-LA}]^{1.0}\cdot[\mathbf{16}]^{1.0}\cdot[\text{BnOH}]^{1.0} \quad (1)$$

The reasons for the apparent difference in the dependence on catalyst concentration observed for **10** and **16** (rate orders in catalyst = 1.2 and 1.0, respectively) and its true significance are unclear at this stage. It possibly reflects a tendency to aggregation in the former case,[8b,55,57] whereas **16** is probably monomeric in solution. Note also that in contrast with our results, Cui et al. reported a kinetic order in initiator (triethanolamine) of −0.352 for the *i*ROP of *rac*-LA catalyzed by an yttrium complex; however, the authors did not consider the dependency in catalyst concentration in their study.[58]

At fixed concentrations ($[\text{L-LA}]_0$ = 2.0 M, $[\mathbf{16}]_0$ = 14.67 mM, $[\text{BnOH}]_0$ = 96.67 mM, $[\text{L-LA}]_0/[\mathbf{16}]_0/[\text{ROH}]_0$ = 136:1:6.6), the kinetics were examined in the temperature range 85−100 °C in order to determine the activation parameters using the Eyring equation.[59] In each case, first-order kinetics in monomer were observed without induction period. The apparent rate constants were extracted from the semilogarithmic plot of monomer conversion versus reaction time (see the Supporting Information), and the activation parameters $\Delta H^{\ddagger}$ = 14.8(5) kcal·$\text{mol}^{-1}$ and $\Delta S^{\ddagger} = -7.6(2.0)$ cal·$\text{K}^{-1}$·$\text{mol}^{-1}$ were calculated from the plot of $\ln(k_{app}/T)$ versus $1/T$ (Figure 9). The value for the enthalpy of activation for the ROP of L-LA promoted by **16**/BnOH is in the upper range of values (7 to 12 kcal·$\text{mol}^{-1}$)


dx.doi.org/10.1021/ja2024977 |*J. Am. Chem. Soc.* 2011, 133, 9069–9087

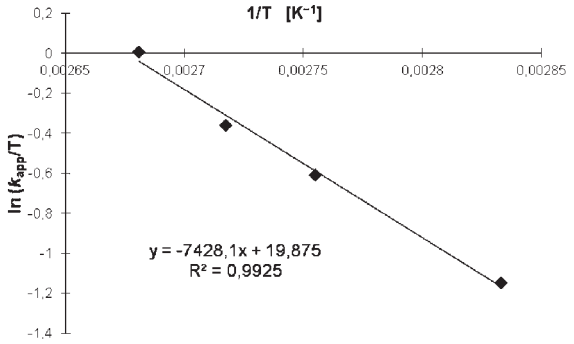


**Figure 9.** Eyring plot for the determination of activation parameters for the polymerization of L-LA promoted by **16**/BnOH. $[\text{L-LA}]_0$ = 2.0 M, $[\mathbf{16}]_0$ = 14.67 mM, $[\text{BnOH}]_0$ = 96.67 mM, $[\text{L-LA}]_0/[\mathbf{16}]_0/[\text{ROH}]_0$ = 136:1:6.6. Polymerizations carried out in toluene-$d_8$ in the temperature range 85−100 °C.

reported for complexes operating according to a coordination−insertion mechanism (in the absence of external nucleophile), while the value found for the entropy of activation is at the lower end of those reported for these systems (ca. −8 to −36 cal·K$^{-1}$·mol$^{-1}$).[7a,10f,60] The higher activation parameters found for **16**/BnOH are not unexpected because (i) it proceeds according to the so-called activated monomer mechanism, and (ii) **16**/BnOH is a *binary* catalyst, as opposed to the single-component initiators described elsewhere.[7a,10f,60]

The apparent rate constants for the *i*ROP of L-LA catalyzed by addition of BnOH to **13**−**17** were determined by NMR in toluene-$d_8$ under rigorously identical experimental conditions (100 °C, $[\text{L-LA}]_0$ = 2.0 M, $[\text{L-LA}]_0/[\text{Met}]_0/[\text{ROH}]_0$ = 136:1:6.6). As found earlier, the Mg derivative **14** exhibited hardly any catalytic activity under these conditions. By contrast, apparent rate constants of 0.0001, 0.0004, 0.0013, and 0.0014 s$^{-1}$ were calculated for **13**, **15**, **16**, and **17**, respectively. The catalytic activity hence varies in the order Mg ≪ Zn < Ca < Sr ≈ Ba, that is, it increases with the ionic radius of the metal. This is in agreement with the observations made previously with large scale polymerizations performed in Schlenk flasks and also follows the trend noticed with complexes **8**−**12** supported by the aryloxide ligand $\{\text{LO}^3\}^-$.[33,61]

**DFT Calculations.** In order to gain some insight on the structure and reactivity of these two families of complexes, theoretical investigations were carried out at the DFT(B3PW91) level. First, the suitability of the method was assessed by comparing the optimized calculated geometries of all $\{\text{LO}^3\}\text{M}^+$ and $\{\text{RO}^3\}\text{M}^+$ compounds (M = Mg, Ca, Sr, Ba, and Zn) with the available solid-state structures determined experimentally. In all cases, only the monomeric complex without any counterion ($\mathbf{8}^+$−$\mathbf{12}^+$ and $\mathbf{13}^+$−$\mathbf{17}^+$) was considered in order to reduce calculation times. We found that the optimized structures matched adequately the experimental ones, and in particular, the calculations confirmed the presence of stabilizing Ae···F contacts in $\mathbf{15}^+$−$\mathbf{17}^+$. In fact, all attempts to optimize geometries without these Ae···F interactions proved unsuccessful. As in the X-ray crystal structures, the shortest calculated Ae···F distances were obtained for $\mathbf{16}^+$ (Sr) and then $\mathbf{17}^+$ (Ba), whereas these contacts are weaker in the case of $\mathbf{15}^+$ (Ca) and especially $\mathbf{14}^+$ (Mg); this trend in the alkaline series can be associated with steric effects. The strength of these interactions was quantified by means of NBO using the second-order perturbation analysis. A stabilizing interaction of 40 kcal·mol$^{-1}$ was found for $\mathbf{16}^+$, 25−26 kcal·mol$^{-1}$ for $\mathbf{15}^+/\mathbf{17}^+$, and only 12 kcal·mol$^{-1}$ in the case of $\mathbf{14}^+$. The highest values are in the range of those found for donor−acceptor interactions in ambiphilic complexes,[62] whereas those found for the Mg derivative have the intensity of strong agostic interactions. Another indication of the strength of these interactions is provided by the analysis of the Wiberg indexes. In agreement with the interaction energies, the Wiberg indexes decrease from Sr (0.12) to Mg (0.06) with an intermediate value of 0.09 for both Ca and Ba. Similar Wiberg indexes were reported in the case of metal−metal ($d^8$−$d^8$) interactions by Bercaw et al.[63]

For all complexes, the calculated positive charge on the metal (Table 3) is close to the expected oxidation state (between +1.32 and +1.49 for $\mathbf{8}^+$−$\mathbf{12}^+$ and +1.28 and +1.45 for $\mathbf{13}^+$−$\mathbf{17}^+$). In a given series ($\mathbf{8}^+$−$\mathbf{12}^+$ versus $\mathbf{13}^+$−$\mathbf{17}^+$), the observed variation for the calculated charge with the nature of the metal is rather unclear, as it does not clearly reflect the evolution of the Lewis acidity and electroposivity. However, the two trends follow the same relative pattern, independently of the nature of the supporting ligand.

The method was then used to shed light on the results of *i*ROP of L-LA. Despite our efforts, it has not been possible so far to locate any transition state for the reaction of L-LA with an external alcohol (namely, MeOH), and work is still in progress in that direction. However, some interesting features can be derived by analyzing the coordination of the monomer as well as the thermodynamics of the reaction. Within each series, the coordination energy of L-LA to the metal center varies according to the metal charge. The coordination of L-LA is endergonic in the case of small variations of the charge ($|\delta_{\text{charge}}| < 0.06$), while it is exergonic with larger $\delta_{\text{charge}}$ (Table 3). This is particularly striking in the case of complexes $\mathbf{15}^+$−$\mathbf{17}^+$, where substantial coordination energies ($-6.4 < \Delta G < -11.2$ kcal·mol$^{-1}$) and decrease of the charge on the metal ($-0.04 < \delta_{\text{charge}} < -0.16$) were computed. This may be related to the presence of Ae···F interactions in these complexes. Indeed, upon coordination of L-LA, the Ae···F distances increased by ca. 0.2 Å with respect to their initial values in $\mathbf{15}^+$−$\mathbf{17}^+$. Besides, generally larger variations (both for the positive charge on the metal and the coordination energy) were observed in the case of complexes supported by $\{\text{RO}^3\}^-$ in comparison to those bearing $\{\text{LO}^3\}^-$. Finally, in both series, the magnitudes of $\Delta G$ and $\delta_{\text{charge}}$ increased clearly with the electropositive nature of the metal; this is in excellent agreement with the experimental data, which unambiguously showed an increase in catalytic activity with the metal size. The case of the Ca complex **15** is somewhat specific since the variation of the charge is rather limited ($\delta_{\text{charge}} = -0.04$), and yet the coordination of the monomer is clearly energetically favorable ($\Delta G = -6.4$ kcal·mol$^{-1}$). This may reflect the subtle balance between size of the metal (and electropositivity of the element) and stabilization through Ae···F internal interactions in this family of complexes.The cases of Mg derivatives $\mathbf{9}^+$ and $\mathbf{14}^+$ stand out, as the highly endergonic coordination of L-LA (+11.2 and +9.6 kcal·mol$^{-1}$, respectively) can be correlated to the inability of these two complexes to promote the *i*ROP of L-LA. Even if the coordination of the monomer on the Zn cation $\mathbf{8}^+$ ($\Delta G$ = +15.0 kcal·mol$^{-1}$) seems less favorable than on its Mg counterpart $\mathbf{9}^+$ ($\Delta G$ = +11.2 kcal·mol$^{-1}$), coordination of the opened monomer (following the first ring opening after nucleophilic attack by MeOH) onto the metal center is clearly much more energetically costly in the latter case ($\Delta G$ = +1.2 and +15.1 kcal·mol$^{-1}$ for $\mathbf{8}^+$ and $\mathbf{9}^+$, respectively). This may account for the observed differences in the catalytic ability of these two


dx.doi.org/10.1021/ja2024977 |*J. Am. Chem. Soc.* 2011, 133, 9069–9087

**Table 3. Calculated (DFT(B3PW91) Level) Charges, Coordination Energies, and Variations of the Charge in Complexes $8^+-17^+$ and Their Adducts after Coordination of L-Lactide and the Product of Opening of L-LA by MeOH**

| | initial complex | | | L-LA adduct[a] | | | | L-LA opened by MeOH–chelate[b] | | | |
|---|---|---|---|---|---|---|---|---|---|---|---|
| | $\{LO^3\}^-8^+-12^+$ | $\{RO^3\}^-13^+-17^+$ | | $\{LO^3\}^-$ | | $\{RO^3\}^-$ | | $\{LO^3\}^-$ | | $\{RO^3\}^-$ | |
| | charge | charge | $\Delta G^c$ [kcal·mol$^{-1}$] | charge ($\delta_{charge}$)[d] | $\Delta G^c$ [kcal·mol$^{-1}$] | charge ($\delta_{charge}$)[d] | $\Delta G^c$ [kcal·mol$^{-1}$] | charge ($\delta_{charge}$)[d] | $\Delta G^c$ [kcal·mol$^{-1}$] | charge ($\delta_{charge}$)[d] | |
| Zn | +1.32 | +1.28 | 15.0 | +1.29 (−0.03) | 2.0 | +1.28 (0.00) | 1.2 | +1.32 (0.00) | 8.0 | +1.31 (+0.03) | |
| Mg | +1.47 | +1.42 | 11.2 | +1.44 (−0.03) | 9.6 | +1.41 (−0.01) | 15.1 | +1.54 (+0.07) | 9.3 | +1.45 (+0.03) | |
| Ca | +1.49 | +1.43 | 1.1 | +1.43 (−0.06) | −6.4 | +1.39 (−0.04) | 3.8 | +1.44 (−0.05) | −5.6 | +1.40 (−0.03) | |
| Sr | +1.31 | +1.34 | −2.5 | +1.23 (−0.08) | −11.2 | +1.18 (−0.16) | −4.9 | +1.16 (−0.15) | −14.3 | +1.06 (−0.28) | |
| Ba | +1.39 | +1.45 | −3.8 | +1.30 (−0.09) | −10.7 | +1.31 (−0.14) | −8.4 | +1.21 (−0.18) | −15.9 | +1.16 (−0.29) | |

[a] Adduct between L-LA and complexes $8^+-17^+$. [b] Adduct (chelating form) between the product resulting from the opening of L-LA by MeOH and complexes $8^+-17^+$. [c] Variation of free energy with respect to the initial complexes $8^+-17^+$. [d] Charge and variation of the positive charge with respect to the initial complexes $8^+-17^+$.

complexes, as unlike $9^+$, the Zn complex $8^+$ is somewhat active at high temperature (100 °C). In fact, ring opening of coordinated L-LA seems to be clearly disfavored in the case of $9^+$ (compare the coordination energies of L-LA, $\Delta G = +11.2$ kcal·mol$^{-1}$, and that of the opened product, $\Delta G = +15.1$ kcal·mol$^{-1}$).

Similar behaviors were also observed upon coordination onto the metal centers of $CH_3O-C(O)-CH(CH_3)-O-C(O)-CH(CH_3)-OH$ (i.e., the product resulting from the opening of L-LA by nucleophilic attack of MeOH) with concomitant formation of a chelating adduct (Table 3). The formation of a chelate (by coordination of the hydroxyl and one carbonyl groups) is found to be particularly stabilizing in the cases of the larger metals Sr and Ba.

## CONCLUSIONS AND PERSPECTIVES

We have devised original and efficient routes for the synthesis of well-defined, solvent-free cationic complexes of the large alkaline-earth metals, magnesium and zinc. This has given access for the first time to the preparation of two whole families of discrete aryloxide and fluorinated alkoxide cations of these metals.

The importance of the chelating ability of the ligand system for the stabilization of the cations is crucial, especially when the size of the metal center increases. Additional, strong secondary Ae···F interactions (detected in the solid state and estimated to be 12−40 kcal·mol$^{-1}$ by DFT calculations) between the metal (Ca, Sr, Ba) and fluorine atoms in $\{RO^3\}^-$ further contribute to the stabilization of these extremely electrophilic species. It is interesting to note that in all of our studies of complexes of zinc, aluminum, or early transition metals supported by fluorinated tertiary alkoxides,[39] only one occurrence of weak M···F interaction was identified, in the case of yttrium (Y···F = 2.806(2) Å).[64] On the other hand, the present work provides further evidence that they are readily and significantly involved in the stabilization of electrophilic complexes of Ca, Sr, and Ba.[21d,27f,36d,47−49] These Ae···F interactions may reflect lower $\pi$-donating ability for the fluorinated alkoxide and/or a further need from the metal in these species for electron density which can only be (partly) supplied by the F atoms in $\{RO^3\}^-$.

Because they are associated with a weakly coordinating counterion and do not contain external Lewis bases such as THF, the Ca, Sr, and Ba cations constitute rare examples of very good Ae catalysts for the controlled *i*ROP of L-LA upon addition of an external nucleophilic initiator such as *i*PrOH or BnOH. The activity of these binary systems compare for instance favorably with that of the tetrahydroborate Ca cations recently reported by Mountford.[34] The most active systems based on Sr and Ba can operate at room temperature. The kinetics exhibit first-order dependence on all components of the system in the case of the *i*ROP of L-LA promoted by **16**/BnOH, suggesting that all three components are involved in the rate-determining step. This is in line with the spectroscopic observations that **16** does not interact with L-LA or BnOH by themselves but promotes the opening of L-LA upon addition of 1 equiv of alcohol versus the monomer. However, attempts to localize transition states during the ring opening of coordinated L-LA by MeOH have so far been unsuccessful owing to the complexity of these systems.

The Ae complexes **15**−**17**, supported by the fluorinated ligand $\{RO^3\}^-$, are clearly less active than their aryloxide analogues **10**−**12**; this likely arises from the presence of internal secondary Ae···F interactions in **15**−**17**, although $^{19}F\{^1H\}$

**Scheme 3. Traditional Activated Monomer Mechanism (from ref 33) for the Immortal ROP of L-LA Catalyzed by a Binary Catalyst $Met^+$/ROH ($Met^+$ = Lewis acidic metal)**

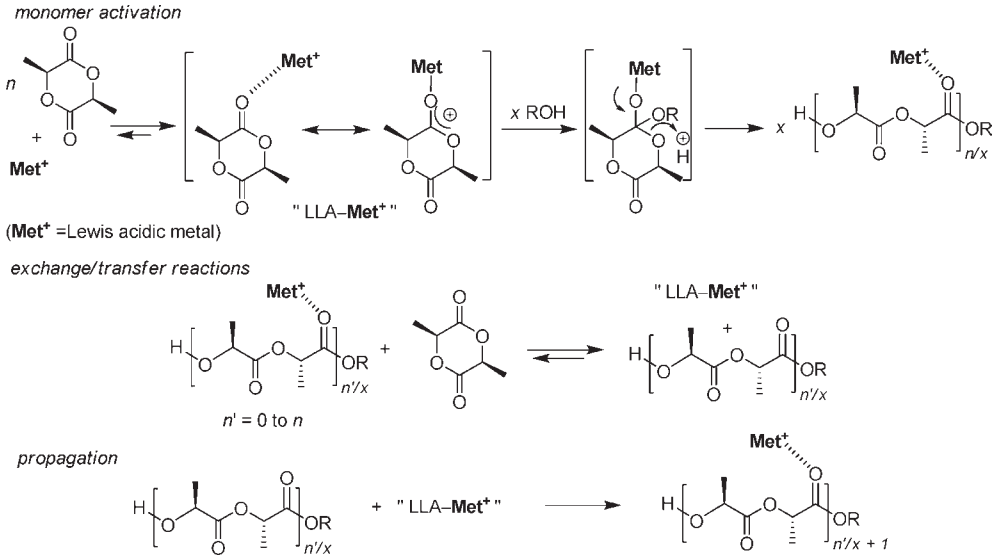


NMR spectroscopy does not provide definitive evidence that these interactions persist in solution (note that, to our knowledge, the persistence in solution of secondary Ae···F contacts identified in the solid state has never been demonstrated previously in neutral complexes,[21d,27f,47] while there is no precedent of similar interactions in well-defined Ae cationic complexes). NMR and preparative scale experiments have shown that complexes **16** and **17** are perfectly stable at room temperature in the presence of L-LA or BnOH; it is possible that although thermodynamically favorable (see calculations), the coordination of L-LA on the metal is kinetically unfavorable because of the fluorine interactions.

The reasons for the observed order of activity (Ba ≈ Sr > Ca > Zn ≫ Mg) are still unclear. On the basis of the Lewis acidity of the metal, which should be a prominent feature in an activated monomer mechanism, where the monomer is activated by the Lewis acidic metal center (Scheme 3), the opposite trend, that is, the Mg and Ba derivatives as the most and least active catalysts, respectively, might have been expected. However, the catalytic activity increases in line with the size and the electropositivity of the metal, an experimental observation corroborated by DFT calculations. It may well be that the smaller metals are deactivated by the very chelating $\{LO^3\}^-$ and $\{RO^3\}^-$ ligands, either simply because no coordination sites are available for the incoming monomer or because the aza-15-crown-5 macrocycle binds more tightly in the cases of the most Lewis acidic metals. However, caution is required for the selection of the ligand framework, as demonstrated by (i) the failure to synthesize cationic complexes supported by the tridentate ligand $\{LO^1\}^-$ and (ii) the high catalytic efficiency but poor control displayed by **5** and **6**, where the metal is supported by the tetradentate $\{LO^2\}^-$ and additional THF.

The rational design of well-defined, solvent-free Ae cations opens the door to the comprehensive investigation of their reactivity. Current efforts in our group aim particularly at rationalizing these observations by designing complexes supported by new ancillary ligands and by the means of theoretical calculations. A correct assessment of the behavior of these cationic complexes will necessarily involve the accurate determination of their nuclearity in solution, which has so far been impeded by their poor solubility in common deuterated solvents used for PGSE NMR studies.

## EXPERIMENTAL SECTION

**General Procedures.** Full experimental and analytical protocols are given in the Supporting Information. $[H(OEt_2)_2^+][H_2N\{B(C_6F_5)_3\}_2]^-$[40a] $[\{LO^3\}HH^+][H_2N\{B(C_6F_5)_3\}_2]^-$ (**3**),[33] $[\{LO^3\}M^+][H_2N\{B(C_6F_5)_3\}_2]^-$ (M = Zn, **8**; Mg, **9**; Ca, **10**; Sr, **11**; Ba, **12**),[33] $Zn[N(SiMe_3)_2]_2$,[65] $\{Mg[N(SiMe_3)_2]_2\}_2$,[66] $Ca[N(SiMe_3)_2]_2(THF)_2$,[19c] $Sr[N(SiMe_3)_2]_2(THF)_2$,[67] $Ba[N(SiMe_3)_2]_2(THF)_2$,[67] $\{LO^1\}H$,[8n] $\{LO^2\}H$,[43] and $\{LO^3\}H$[32] were prepared as described in the literature. Isopropanol and benzyl alcohol employed for polymerization purposes (HPLC grade, VWR) were dried and distilled over dry magnesium turnings and then stored over 3 Å molecular sieves. L-lactide (L-LA) was provided by Total Petrochemicals and purified by recrystallized from a hot, concentrated *i*PrOH solution (80 °C), followed by two subsequent recrystallizations in hot toluene (105 °C).

NMR spectra were recorded on Bruker AC-200, AC-300, AC-400, and AM-500 spectrometers. All chemicals shifts were determined using residual signals of the deuterated solvents and were calibrated versus $SiMe_4$. $^{19}F\{^1H\}$ chemical shifts were determined by external reference to an aqueous solution of NaBF4.

Size exclusion chromatography (SEC) measurements were performed on a Polymer Laboratories PL-GPC 50 instrument equipped with a PLgel 5 Å MIXED-C column and a refractive index detector. The GPC column was eluted with THF at room temperature at 1 mL/min and was calibrated using 11 monodisperse polystyrene standards in the range of 580−380 000 g·mol$^{-1}$. The molecular weights of all PLAs were corrected by a factor of 0.58.[52]

MALDI-TOF mass spectra were obtained with a Bruker Daltonic MicroFlex LT, using a nitrogen laser source (337 nm, 3 ns) in linear mode with a positive acceleration voltage of 20 kV. Bruker Care Peptide Calibration Standard and Protein Calibration Standard I were used for external calibration.

**2-[(1,4,7,10-Tetraoxa-13-azacyclopentadecan-13-yl)methyl]-1,1,1,3,3,3-hexafluoropropan-2-ol ($\{RO^3\}H$).** A solution of 1-aza-15-crown-5 (5.89 g, 26.9 mmol) in $Et_2O$ (100 mL) was added dropwise at 0 °C


dx.doi.org/10.1021/ja2024977 |J. Am. Chem. Soc. 2011, 133, 9069–9087

to a solution of 3,3,3-trifluoro-2-(trifluoromethyl)-1,2-propenoxide (4.84 g, 26.9 mmol) in $Et_2O$ (350 mL). The resulting colorless solution was allowed to warm slowly to room temperature, and stirring was pursued overnight. The solution was then concentrated to 60 mL and washed with a saturated aqueous solution of $NaHCO_3$ (2 × 150 mL). The aqueous layers were back-extracted with $Et_2O$ (70 mL). The organic layers were combined and dried over $MgSO_4$, and the solvent was removed under vacuum to afford $\{\mathbf{RO^3}\}\mathbf{H}$ as a colorless oil that was dried to constant weight. The oil slowly solidified upon storage at +4 °C. Yield 8.15 g (76%). $^1$H NMR ($CDCl_3$, 500.13 MHz, 298 K): $\delta$ 6.46 (br s, 1H, O*H*), 3.63−3.61 (m, 4H, O−C$H_2$), 3.59−3.56 (m, 12H, O-C$H_2$), 3.07 (s, 2H, C$H_2$-C$(CF_3)_2$), 2.87 (t, $^3J_{HH}$ = 5.2, 4H, N-C$H_2$-$CH_2$) ppm. $^{13}$C{$^1$H} NMR ($CDCl_3$, 125.76 MHz, 298 K): $\delta$ 123.5 (q, $^1J_{CF}$ = 283, $CF_3$), 73.0 (hept, $^2J_{CF}$ = 29, $C(CF_3)_2$), 70.9, 70.3, 70.2, 69.2 (all O-$CH_2$), 57.2 (N-$CH_2$-$CH_2$), 55.2 (N-$CH_2$-C$(CF_3)_2$OH) ppm. $^{19}$F-{$^1$H} NMR ($CDCl_3$, 188.29 MHz, 298 K): $\delta$ −77.4 (s, 6F, C$(CF_3)_2$) ppm. Anal. Calcd for $C_{14}H_{23}F_6NO_5$ (399.33 g·mol$^{-1}$): C 42.1, H 5.8, N 3.5. Found: C 42.3, H 6.0, N 3.4.

**$[\{\mathbf{LO^1}\}\mathbf{HH}]^+[\mathbf{H_2N}\{\mathbf{B(C_6F_5)_3}\}_2]^-$ (1).** $[H(OEt_2)_2]^+[H_2N\{B(C_6F_5)_3\}_2]^-$ (1.20 g, 1.01 mmol) was added in fractions with a bent finger to a colorless solution of $\{\mathbf{LO^1}\}\mathbf{H}$ (0.31 g, 1.01 mmol) in $Et_2O$ (30 mL). The resulting pale yellow solution was stirred at room temperature for 2 h. An oily material formed upon addition of pentane (120 mL). The supernatant was removed by filtration, and the oil was dried in vacuo to yield a colorless solid that was further washed with pentane (2 × 25 mL). After drying under vacuum, **1** was isolated as a fine white powder. Yield 1.10 g (82%). X-ray quality crystals were grown by recrystallization from a dichloromethane/pentane mixture at −26 °C. $^1$H NMR ($CD_2Cl_2$, 500.13 MHz, 298 K): $\delta$ 7.54 (d, $^4J_{HH}$ = 2.5, 1H, arom-*H*), 7.13 (d, $^4J_{HH}$ = 2.5, 1H, arom-*H*), 6.79 (br s, 1H, O*H*), 5.78 (br s, 1H, N$H^+$), 5.73 (br, 2H, N$H_2$), 4.38 (s, 2H, Ar-C$H_2$-N), 4.24 (dd, $^2J_{HH}$ = 12.5, 2H, C*H*(H)-O), 3.76 (dt, $^2J_{HH}$ = 12.5, 2H, C(H)*H*-O), 3.51 (dd, $^2J_{HH}$ = 12.5, 2H, $CH_2$-C*H*(H)-N), 3.23 (m, 2H, $CH_2$-C(H)*H*-N), 1.47 (s, 9H, *p*-C$(CH_3)_3$), 1.30 (s, 9H, *o*-C$(CH_3)_3$) ppm. $^{13}$C{$^1$H} NMR ($CD_2Cl_2$, 125.76 MHz, 298 K): $\delta$ 149.8, 146.7, 141.2, 138.8, 137.9, 135.4 (all $C_6F_5$), 150.1 (*i*-*C*), 146.3 (*o*-*C*), 135.8 (*p*-*C*), 128.2 (*m*-*C*), 126.9 (*m*-*C*), 114.2 (*o*-*C*), 62.0 (Ar-$CH_2$-N), 64.7 (O-$CH_2$), 53.2 (N-$CH_2$-$CH_2$), 34.4 (*p*-C$(CH_3)_3$), 34.2 (*o*-C$(CH_3)_3$), 31.2 (*o*-C$(CH_3)_3$), 30.5 (*p*-C$(CH_3)_3$) ppm. $^{19}$F{$^1$H} NMR ($CD_2Cl_2$, 188.29 MHz, 298 K): $\delta$ −133.4 (d, $^3J_{FF}$ = 18.9, 12F, *o*-F), −160.5 (t, $^3J_{FF}$ = 18.9, 6F, *p*-F), −166.1 (d, $^3J_{FF}$ = 18.9, 12F, *m*-F) ppm. $^{11}$B NMR (96.29 MHz, $CD_2Cl_2$, 298 K): $\delta$ −8.4 ppm. Anal. Calcd for $C_{55}H_{34}B_2F_{30}N_2O_2$ (1346.23 g·mol$^{-1}$): C 49.1, H 2.6, N 2.1. Found: C 49.1, H 2.6, N 2.2.

**$[\{\mathbf{LO^2}\}\mathbf{HH}]^+[\mathbf{H_2N}\{\mathbf{B(C_6F_5)_3}\}_2]^-$ (2).** In an manner analogous to that described for **1**, $[H(OEt_2)_2]^+$ $[H_2N\{B(C_6F_5)_3\}_2]^-$ (0.92 g, 0.77 mmol) and $\{\mathbf{LO^2}\}\mathbf{H}$ (0.32 g, 0.91 mmol) were reacted in $Et_2O$ (25 mL) to give a foamy material after removal of the solvent. This solid was purified twice by dissolving it in dichloromethane and reprecipitating it by addition of pentane, thus ensuring that all residual $Et_2O$ was eliminated. Drying in vacuo afforded **2** as a colorless powder. Yield 0.65 g (61%). $^1$H NMR ($CD_2Cl_2$, 500.13 MHz, 298 K): $\delta$ 7.73 (br s, 1H, O*H*), 7.52 (d, $^4J_{HH}$ = 2.5, 1H, arom-*H*), 7.13 (d, $^4J_{HH}$ = 2.5, 1H, arom-*H*), 5.71 (br, 2H, N$H_2$), 5.60 (br s, 1H, N$H^+$), 4.38 (s, 2H, Ar-C$H_2$-N), 3.69 (br s, 4H, O-C$H_2$), 3.42 (s, 6H, O-C$H_3$), 3.36 (t, $^3J_{HH}$ = 5.0, 4H, N-C$H_2$-$CH_2$), 1.49 (s, 9H, *o*-C$(CH_3)_3$), 1.32 (s, 9H, *p*-C$(CH_3)_3$) ppm. $^{13}$C{$^1$H} NMR ($CD_2Cl_2$, 125.76 MHz, 298 K): $\delta$ 149.3, 147.3, 140.5, 138.6, 138.0, 136.1 (all $C_6F_5$), 150.5 (*i*-*C*), 145.7 (*p*-*C*), 135.8 (*o*-*C*), 127.6 (*m*-*C*), 127.0 (*m*-*C*), 115.9 (*o*-*C*), 65.0 (O-$CH_2$), 59.6 (O-$CH_3$), 58.8 (Ar-$CH_2$-N), 54.7 (N-$CH_2$-$CH_2$), 34.8 (*p*-C$(CH_3)_3$), 34.3 (*o*-C$(CH_3)_3$), 31.4 (*p*-C$(CH_3)_3$), 30.5 (*o*-C$(CH_3)_3$) ppm. $^{19}$F{$^1$H} NMR ($CD_2Cl_2$, 188.29 MHz, 298 K): $\delta$ −133.4 (d, $^3J_{FF}$ = 18.9, 12F, *o*-F), −160.5 (t, $^3J_{FF}$ = 18.9, 6F, *p*-F), −166.1 (d, $^3J_{FF}$ = 18.9, 12F, *m*-F) ppm. $^{11}$B NMR (96.29 MHz, $CD_2Cl_2$, 298 K): $\delta$ −8.4 ppm. Anal. Calcd for $C_{57}H_{40}F_{30}N_2O_3$ (1392.52 g·mol$^{-1}$): C 49.2, H 2.9, N 2.0. Found: C 49.6, H 2.8, N 1.8.

**$[\{\mathbf{RO^3}\}\mathbf{HH}]^+[\mathbf{H_2N}\{\mathbf{B(C_6F_5)_3}\}_2]^-$ (4).** In a way identical to that described for **2**, the reaction of $[H(OEt_2)_2]^+[H_2N\{B(C_6F_5)_3\}_2]^-$ (5.96 g, 5.01 mmol) and $\{\mathbf{RO^3}\}\mathbf{H}$ (2.00 g, 5.01 mmol) was carried out in $Et_2O$ (100 mL) to give **4** as a colorless powder. Yield 6.50 g (90%). $^1$H NMR ($CD_2Cl_2$, 400.13 MHz, 298 K): $\delta$ 8.0−7.0 (br, 2H, O*H* + N$H^+$), 5.70 (br, 2H, N$H_2$), 3.89 (m, 4H, O-C$H_2$), 3.84 (s, 2H, N-C$H_2$-C$(CF_3)_2$OH), 3.73 (m, 12H, O-C$H_2$), 3.59 (m, 4H, N-C$H_2$-$CH_2$) ppm. $^{13}$C{$^1$H} NMR ($CD_2Cl_2$, 100.61 MHz, 298 K): $\delta$ 149.5, 147.2, 140.7, 138.3 (2 overlapping signals), 135.9 (all $C_6F_5$), 122.2 (q, $^1J_{CF}$ = 284, $CF_3$), 74.3 (hept, $^2J_{CF}$ = 31, $C(CF_3)_2$), 70.2, 69.5, 69.1 (all O-$CH_2$-$CH_2$-O), 63.4 (O-$CH_2$-$CH_2$-N), 59.0 (N-$CH_2$-$CH_2$-O), 55.5 (N-$CH_2$-C$(CF_3)_2$OH) ppm. $^{19}$F{$^1$H} NMR ($CD_2Cl_2$, 188.29 MHz, 298 K): $\delta$ −77.5 (s, 6F, C$(CF_3)_2$), −133.4 (d, $^3J_{FF}$ = 18.9, 12F, *o*-F), −160.6 (t, $^3J_{FF}$ = 18.9, 6F, *p*-F), −166.1 (d, $^3J_{FF}$ = 18.9, 12F, *m*-F) ppm. $^{11}$B NMR (96.29 MHz, $CD_2Cl_2$, 298 K): $\delta$ −8.4 ppm. Anal. Calcd for $C_{50}H_{26}B_2F_{36}N_2O_5$ (1440.31 g·mol$^{-1}$): C 41.7, H 1.8, N 1.9. Found: C 41.4, H 1.9, N 2.0.

**$[\{\mathbf{LO^2}\}\mathbf{Ca(THF)_{0.5}}]^+[\mathbf{H_2N}\{\mathbf{B(C_6F_5)_3}\}_2]^-$ (5).** *Method A.* A solution of **2** (0.30 g, 0.21 mmol) in $Et_2O$ (10 mL) was added dropwise at room temperature to a solution of $Ca[N(SiMe_3)_2]_2(THF)_2$ (0.11 g, 0.22 mmol) in $Et_2O$ (10 mL). The resulting solution was stirred for 3 h, and a white solid was then precipitated upon addition of a large volume of pentane. The solid was purified (3 times) by dissolving it in dichloromethane and then reprecipitating it by addition of pentane to give **5** as a colorless powder that was dried under vacuum to constant weight. Yield 0.22 g (70%).

*Method B.* A solution of $H(OEt)_2^+\cdot NH_2\{B(C_6F_5)_3\}_2^-$ (0.45 g, 0.38 mmol) in $Et_2O$ (10 mL) was added dropwise at room temperature to a solution of **7** (0.21 g, 0.38 mmol) in $Et_2O$ (15 mL) in the presence of a small amount of THF. The colorless solution was stirred at room temperature for 1.5 h, and the volatiles were removed under vacuum. The resulting oil was dissolved in $CH_2Cl_2$ (2 mL), and an oily material formed again by slow addition of pentane (20 mL). The supernatant was transferred out, and the residue was further washed with pentane (2 × 15 mL) to give **5** as a white powder that was dried in vacuo. Yield 0.42 g (77%). $^1$H NMR ($CD_2Cl_2$, 500.13 MHz, 298 K): $\delta$ 7.48 (d, $^4J_{HH}$ = 2.5, 1H, arom-*H*), 7.09 (d, $^4J_{HH}$ = 2.5, 1H, arom-*H*), 5.70 (br, 2H, $NH_2$), 4.40 (br s, 1H, Ar-C*H*(H)-N), 4.14 (br s, 1H, Ar-C(H)*H*-N), 3.77 (br s, 2H, $CH_2$-C$H_2$-O), 3.66 (br, 2H, O-C$H_2$(THF)), 3.45 (s, 6H, O-C$H_3$), 3.10 (br s, 2H, $CH_2$-C$H_2$-O), 2.85 (br, 2H, N-C$H_2$-$CH_2$), 2.40 (br, 2H, N-C$H_2$-$CH_2$), 1.95 (br, 2H, O-$CH_2$-C$H_2$(THF)), 1.55 (s, 9H, *o*-C$(CH_3)_3$), 1.30 (s, 9H, *p*-C$(CH_3)_3$) ppm. $^{13}$C{$^1$H} NMR ($CD_2Cl_2$, 125.76 MHz, 298 K): $\delta$ 149.2, 147.3, 138.5, 138.2, 136.0, 135.9 (all $C_6F_5$), 158.5 (*i*-C), 140.4 (*p*-C), 136.2 (*o*-C), 128.2 (*m*-C), 126.6 (*m*-C), 123.7 (*o*-C), 70.7 (N-$CH_2$-$CH_2$-O), 70.0 (O-$CH_2$(THF)), 61.4 (Ar-$CH_2$-N), 61.0 (O-$CH_3$), 55.7 (N-$CH_2$-$CH_2$), 35.8 (*o*-C$(CH_3)_3$), 34.5 (*p*-C$(CH_3)_3$), 31.7 (*p*-C$(CH_3)_3$), 31.5 (*o*-C$(CH_3)_3$), 25.6 (O-$CH_2$-$CH_2$(THF)) ppm. $^{19}$F{$^1$H} NMR ($CD_2Cl_2$, 188.29 MHz, 298 K): $\delta$ −133.3 (d, $^3J_{FF}$ = 18.9, *o*-F), −160.6 (t, $^3J_{FF}$ = 18.9, *p*-F), −166.1 (t, $^3J_{FF}$ = 18.9, *m*-F) ppm. $^{11}$B NMR ($CD_2Cl_2$, 96.29 MHz, 298 K): $\delta$ −8.3 ppm. Anal. Calcd for $C_{57}H_{38}B_2CaF_{30}N_2O_3\cdot(C_4H_8O)_{0.5}$ (1466.64 g·mol$^{-1}$): C 48.3, H 2.9, N 1.9. Found: C 47.8, H 2.5, N 1.8.

**$[\{\mathbf{LO^2}\}\mathbf{Sr(THF)}]^+[\mathbf{H_2N}\{\mathbf{B(C_6F_5)_3}\}_2]^-$ (6).** At room temperature, **2** (0.27 g, 0.19 mmol) was added in fractions to a solution of $Sr[N(SiMe_3)_2]_2(THF)_2$ (0.11 g, 0.20 mmol) in $Et_2O$ (15 mL). The resulting pale yellow solution was stirred at room temperature for 48 h, and removal of the volatiles gave an oil that solidified upon drying in vacuo. The solid was washed (3 cycles) by dissolving it in minimal amounts of $CH_2Cl_2$ and then reprecipitating it with pentane. After drying to constant weight, **6** was isolated as a fine white powder. Yield 0.22 g (74%). $^1$H NMR ($CD_2Cl_2$, 500.13 MHz, 298 K): $\delta$ 7.44 (d, $^4J_{HH}$ = 2.5, 1H, arom-*H*), 7.07 (d, $^4J_{HH}$ = 2.5, 1H, arom-*H*), 5.71 (br, 2H, N$H_2$), 4.39 (d, $^3J_{HH}$ = 11.0, 1H, Ar-C*H*(H)-N), 4.14 (m, 1H, O-C*H*(H)-$CH_2$-

N), 3.74 (dt, $^2J_{HH}$ = 11.0, 1H, O-C*H*(H)-CH$_2$-N), 3.62 (m, 1H, O-C(H)*H*-CH$_2$-N), 3.37 (br, 4H, O-C*H*$_2$(THF)), 3.35 (s, 3H, O-C*H*$_3$), 3.27 (s, 3H, O-C*H*$_3$), 3.20−3.05 (m, 3H, Ar-C(H)*H*-N + N-C*H*(H)-CH$_2$ + O-C(H)*H*-CH$_2$-N), 2.78−2.65 (m, 2H, N-C*H*(H)-CH$_2$ + N-C(H)*H*-CH$_2$), 2.25 (dt, $^2J_{HH}$ = 14.5, 1H, N-C(H)*H*-CH$_2$), 1.85 (m, $^3J_{HH}$ = 6.0, 4H, O-CH$_2$-C*H*$_2$(THF)), 1.56 (s, 9H, *o*-C(C*H*$_3$)$_3$), 1.28 (s, 9H, *p*-C(C*H*$_3$)$_3$) ppm. $^{13}$C{$^1$H} NMR (CD$_2$Cl$_2$, 125.76 MHz, 298 K): $\delta$ 149.3, 147.4, 140.6, 138.5, 138.1, 136.1 (all $C_6F_5$), 158.6 (*i*-*C*), 140.4 (*p*-*C*), 136.7 (*o*-*C*), 128.2 (*m*-*C*), 126.3 (*m*-*C*), 123.4 (*o*-*C*), 71.2 (O-*C*H$_2$-CH$_2$-N), 70.8 (O-CH$_2$-*C*H$_2$-N), 69.4 (O-*C*H$_2$(THF)), 60.8 (O-*C*H$_3$), 60.3 (O-*C*H$_3$), 59.3 (Ar-*C*H$_2$-N), 56.2 (N-*C*H$_2$-CH$_2$), 52.3 (N-*C*H$_2$-CH$_2$), 35.6 (*o*-*C*(CH$_3$)$_3$), 34.3 (*p*-*C*(CH$_3$)$_3$), 31.6 (*p*-C(*C*H$_3$)$_3$), 31.4 (*o*-C(*C*H$_3$)$_3$), 25.7 (O-CH$_2$-*C*H$_2$(THF)) ppm. $^{19}$F{$^1$H} NMR (CD$_2$Cl$_2$, 188.29 MHz, 298 K): $\delta$ −133.4 (d, $^3J_{FF}$ = 18.9, 12F, *o*-F), −160.5 (t, $^3J_{FF}$ = 18.9, 6F, *p*-F), −166.1 (d, $^3J_{FF}$ = 18.9, 12F, *m*-F) ppm. $^{11}$B NMR (96.29 MHz, CD$_2$Cl$_2$, 298 K): $\delta$ −8.4 ppm. Anal. Calcd for $C_{57}H_{38}B_2F_{30}N_2O_3Sr\cdot(C_4H_8O)$ (1550.23 g·mol$^{-1}$): C 47.3, H 3.0, N 1.8. Found: C 47.9, H 3.2, N 2.0.

**{LO$^2$}CaN(SiMe$_3$)$_2$ (7).** At room temperature, a solution of {LO$^2$}H (0.34 g, 0.97 mmol) in pentane (10 mL) was added slowly to a solution of Ca[N(SiMe$_3$)$_2$]$_2$(THF)$_2$ (0.51 g, 1.02 mmol) in pentane (15 mL). After 6 h, the reaction solution was concentrated to 2 mL and kept overnight at −30 °C to give **7** as a crystalline solid. Yield 0.39 g (73%). Twinned crystals were afforded by recrystallization from a benzene/pentane mixture at room temperature, and their structure was determined. $^1$H NMR ($C_6D_6$, 500.13 MHz, 298 K): $\delta$ 7.59 (d, $^4J_{HH}$ = 2.6, 1H, arom-*H*), 6.96 (d, $^4J_{HH}$ = 2.6, 1H, arom-*H*), 3.13 (s, 2H, Ar-C*H*$_2$-N), 3.00 (s, 6H, O-C*H*$_3$), 2.83 (m, 2H, CH$_2$-C(H)*H*-O), 2.50 (m, 2H, CH$_2$-C*H*(H)-O), 1.99 (m, 4H, N-C*H*$_2$-CH$_2$), 1.83(s, 9H, *o*-C(C*H*$_3$)$_3$), 1.49(s, 9H, *p*-C(C*H*$_3$)$_3$), 0.43(s, 18H, Si(C*H*$_3$)$_3$) ppm. $^{13}$C{$^1$H} NMR ($C_6D_6$, 125.76 MHz, 298 K): $\delta$ 165.3 (*i*-*C*), 137.4 (*o*-*C*), 133.6 (*p*-*C*), 126.1 (*o*-*C*), 124.7 (*m*-*C*), 122.9 (*m*-*C*), 70.6 (CH$_2$-CH$_2$-O), 60.2 (Ar-*C*H$_2$-N), 60.1 (O-*C*H$_3$), 55.9 (N-*C*H$_2$-CH$_2$), 36.2 (*o*-*C*(CH$_3$)$_3$), 34.6 (*p*-*C*(CH$_3$)$_3$), 33.0 (*p*-C(*C*H$_3$)$_3$), 30.7 (*o*-C(*C*H$_3$)$_3$), 6.4 (Si(*C*H$_3$)$_3$) ppm. Anal. Calcd for $C_{27}H_{54}CaN_2O_3Si_2$ (550.99 g·mol$^{-1}$): C 58.9, H 9.9, N 5.1. Found: C 58.9, H 10.0, N 5.1.

**[{RO$^3$}Zn]$^+$[H$_2$N{B(C$_6$F$_5$)$_3$}$_2$]$^-$ (13).** At room temperature, **4** (1.60 g, 1.11 mmol) was added in fractions with a bent finger to a solution of Zn[N(SiMe$_3$)$_2$]$_2$ (0.47 g, 1.22 mmol) in Et$_2$O (30 mL). A white precipitate formed within minutes. Vigorous stirring was ensured for 1 h, and the precipitate was isolated by filtration. Residual Et$_2$O and HN(SiMe$_3$)$_2$ were fully removed by dissolving the solid in CH$_2$Cl$_2$ and reprecipitating it by addition of pentane (purification step repeated at least 3 times) to yield **13** as a colorless powder which was dried in vacuo to constant weight. Yield 1.20 g (73%). Single-crystals suitable for X-ray diffraction studies (colorless rods) were obtained by recrystallization from CD$_2$Cl$_2$ at room temperature. Alternatively, **13** can also be prepared in high yield with the same procedure by reaction of ZnEt$_2$ and **4**. $^1$H NMR (CD$_2$Cl$_2$, 500.13 MHz, 298 K): $\delta$ 5.70 (br, 2H, N*H*$_2$), 4.25−4.14 (m, 2H, O-C*H*$_2$), 4.10−3.92 (m, 12 H, O-C*H*$_2$), 3.81−3.69 (m, 2H, O-C*H*$_2$-CH$_2$-N), 3.22−3.02 (m, 4H, N-C*H*$_2$-CH$_2$), 3.12 (s, 2H, C*H*$_2$-C(CF$_3$)$_2$O) ppm. $^{13}$C{$^1$H} NMR (CD$_2$Cl$_2$, 125.76 MHz, 298 K): $\delta$ 149.2, 147.4, 140.5, 138.5, 138.1, 136.1 (all $C_6F_5$), 125.2 (q, $^1J_{CF}$ = 290, *C*F$_3$), 77.2 (hept, $^2J_{CF}$ = 27, *C*(CF$_3$)$_2$), 69.5, 67.1, 67.0, 66.7 (all O-*C*H$_2$-*C*H$_2$-O), 57.1 (CH$_2$-*C*(CF$_3$)$_2$O), 55.0 (N-*C*H$_2$-CH$_2$) ppm. $^{19}$F{$^1$H} NMR (CD$_2$Cl$_2$, 188.29 MHz, 298 K): $\delta$ −79.4 (s, 6F, C(*C*F$_3$)$_2$), −133.4 (d, $^3J_{FF}$ = 18.9, 12F, *o*-F), −160.6 (t, $^3J_{FF}$ = 18.9, 6F, *p*-F), −166.1 (d, $^3J_{FF}$ = 18.9, 12F, *m*-F) ppm. $^{11}$B NMR (96.29 MHz, CD$_2$Cl$_2$, 298 K): $\delta$ −8.5 ppm. Anal. Calcd for $C_{50}H_{24}B_2F_{36}N_2O_5Zn$ (1503.68 g·mol$^{-1}$): C 39.9, H 1.6, N 1.9. Found: C 39.7, H 1.9, N 1.9.

**[{RO$^3$}Mg]$^+$[H$_2$N{B(C$_6$F$_5$)$_3$}$_2$]$^-$ (14).** Following the same procedure as that described above for **13**, the Mg derivative **14** was prepared by reaction of **4** (1.03 g, 0.72 mmol) and {Mg[N(SiMe$_3$)$_2$]$_2$}$_2$ (0.25 g, 0.36 mmol) in Et$_2$O (20 mL). Yield 0.80 g (76%). X-ray quality crystals of the colorless **14** were grown from a saturated solution of CD$_2$Cl$_2$ at room temperature. $^1$H NMR (CD$_2$Cl$_2$, 500.13 MHz, 298 K): $\delta$ 5.70 (br, 2H, N*H*$_2$), 4.25−4.17 (m, 2H, O-C*H*$_2$), 4.12−4.05 (m, 2H, O-C*H*$_2$), 4.05−3.94 (m, 10 H, O-C*H*$_2$-C*H*$_2$-O + O-C*H*$_2$-CH$_2$-N), 3.88−3.79 (m, 2H, O-C*H*$_2$-CH$_2$-N), 3.13 (s, 2H, C*H*$_2$-C(CF$_3$)$_2$O), 3.10−2.98 (m, 4H, N-C*H*$_2$-CH$_2$-O) ppm. $^{13}$C{$^1$H} NMR (CD$_2$Cl$_2$, 125.76 MHz, 298 K): $\delta$ 149.2, 147.4, 140.6, 138.5, 138.2, 36.1 (all $C_6F_5$), 125.7 (q, $^1J_{CF}$ = 292, *C*F$_3$), 78.1 (m, *C*(CF$_3$)$_2$), 69.2, 68.2, 67.3, 67.2 (all O-*C*H$_2$-*C*H$_2$-O), 57.8 (CH$_2$-*C*(CF$_3$)$_2$O), 54.8 (N-*C*H$_2$-CH$_2$) ppm. $^{19}$F{$^1$H} NMR (CD$_2$Cl$_2$, 188.29 MHz, 298 K): $\delta$ −79.8 (s, 6F, C(*C*F$_3$)$_2$), −133.4 (d, $^3J_{FF}$ = 18.9, 12F, *o*-F), −160.6 (t, $^3J_{FF}$ = 18.9, 6F, *p*-F), −166.1 (d, $^3J_{FF}$ = 18.9, 12F, *m*-F) ppm. $^{11}$B NMR (96.29 MHz, CD$_2$Cl$_2$, 298 K): $\delta$ −8.4 ppm. Anal. Calcd for $C_{50}H_{24}B_2F_{36}MgN_2O_5$ (1462.60 g·mol$^{-1}$): C 41.0, H 1.6, N 1.9. Found: C 40.3, H 1.1, N 1.7.

**[{RO$^3$}Ca]$^+$[H$_2$N{B(C$_6$F$_5$)$_3$}$_2$]$^-$ (15).** Following the same procedure as that described above for **13**, the colorless Ca derivative **15** was prepared by reaction of **4** (1.38 g, 0.96 mmol) and Ca[N(SiMe$_3$)$_2$]$_2$(THF)$_2$ (0.48 g, 0.95 mmol) in Et$_2$O (20 mL). Yield 1.25 g (88%). Single crystals (colorless rods) of **{15}$_4$·3CD$_2$Cl$_2$** were obtained by recrystallization from CD$_2$Cl$_2$ at room temperature. $^1$H NMR (CD$_2$Cl$_2$, 500.13 MHz, 298 K): $\delta$ 5.69 (br, 2H, N*H*$_2$), 4.18−4.01 (m, 4H, O-C*H*$_2$), 4.00−3.84 (m, 8H, O-C*H*$_2$), 3.84−3.76 (m, 2H, O-C*H*$_2$), 3.76−3.69 (m, 2H, O-C*H*$_2$), 3.06 (s, 2H, C*H*$_2$-C(CF$_3$)$_2$O), 3.12−2.84 (br, 4H, N-C*H*$_2$-CH$_2$-O) ppm. $^{13}$C{$^1$H} NMR (CD$_2$Cl$_2$, 125.76 MHz, 298 K): $\delta$ 149.2, 147.3, 140.5, 138.5, 138.0, 136.0 (all $C_6F_5$), 125.6 (q, $^1J_{CF}$ = 292, *C*F$_3$), 80.6 (m, *C*(CF$_3$)$_2$), 68.9, 68.5, 68.2, 67.6 (all O-*C*H$_2$-*C*H$_2$-O), 55.9 (CH$_2$-*C*(CF$_3$)$_2$O), 54.0 (N-*C*H$_2$-CH$_2$) ppm. $^{19}$F{$^1$H} NMR (CD$_2$Cl$_2$, 188.29 MHz, 298 K): $\delta$ −78.2 (s, 6F, C(*C*F$_3$)$_2$), −133.4 (d, $^3J_{FF}$ = 18.9, 12F, *o*-F), −160.6 (t, $^3J_{FF}$ = 18.9, 6F, *p*-F), −166.1 (d, $^3J_{FF}$ = 18.9, 12F, *m*-F) ppm. $^{11}$B NMR (96.29 MHz, CD$_2$Cl$_2$, 298 K): $\delta$ −8.4 ppm. Anal. Calcd for $C_{50}H_{24}B_2CaF_{36}N_2O_5$ (1478.38 g·mol$^{-1}$): C 40.6, H 1.6, N 1.9. Found: C 40.3, H 1.4, N 1.8.

**[{RO$^3$}Sr]$^+$[H$_2$N{B(C$_6$F$_5$)$_3$}$_2$]$^-$ (16).** Following the same procedure as that described above for **13**, the colorless Sr derivative **16** was prepared by reaction of **4** (2.60 g, 1.80 mmol) and Sr[N(SiMe$_3$)$_2$]$_2$(THF)$_2$ (1.00 g, 1.81 mmol) in Et$_2$O (70 mL). Yield 2.50 g (91%). Colorless, X-ray quality crystals of **{16}$_4$·3CD$_2$Cl$_2$** were grown readily from a CD$_2$Cl$_2$ solution stored at room temperature. . $^1$H NMR (CD$_2$Cl$_2$, 500.13 MHz, 298 K): $\delta$ 5.70 (br, 2H, N*H*$_2$), 4.00−3.78 (m, 16H, O-C*H*$_2$), 3.02 (s, 2H, C*H*$_2$-C(CF$_3$)$_2$O), 2.98−2.85 (m, 4H, N-C*H*$_2$-CH$_2$-O) ppm. $^{13}$C{$^1$H} NMR (CD$_2$Cl$_2$, 125.76 MHz, 298 K): $\delta$ 149.2, 147.3, 140.5, 138.5, 138.1, 136.1 (all $C_6F_5$), 126.2 (q, $^1J_{CF}$ = 290, *C*F$_3$), 80.3 (m, *C*(CF$_3$)$_2$), 69.4, 68.8, 68.6, 68.5 (all O-*C*H$_2$-*C*H$_2$-O), 56.1 (CH$_2$-*C*(CF$_3$)$_2$O), 55.5 (N-*C*H$_2$-CH$_2$) ppm. $^{19}$F{$^1$H} NMR (CD$_2$Cl$_2$, 188.29 MHz, 298 K): $\delta$ −78.0 (s, 6F, C(*C*F$_3$)$_2$), −133.4 (d, $^3J_{FF}$ = 18.9, 12F, *o*-F), −160.6 (t, $^3J_{FF}$ = 18.9, 6F, *p*-F), −166.1 (d, $^3J_{FF}$ = 18.9, 12F, *m*-F) ppm. $^{11}$B NMR (96.29 MHz, CD$_2$Cl$_2$, 298 K): $\delta$ −8.4 ppm. Anal. Calcd for $C_{50}H_{24}B_2F_{36}N_2O_5Sr$ (1525.92 g·mol$^{-1}$): C 39.4, H 1.6, N 1.8. Found: C 38.8, H 1.9, N 1.9.

**[{RO$^3$}Ba]$^+$[H$_2$N{B(C$_6$F$_5$)$_3$}$_2$]$^-$ (17).** At room temperature, **4** (1.04 g, 0.72 mmol) was added in fractions to a solution of Ba[N(SiMe$_3$)$_2$]$_2$(THF)$_2$ (0.44 g, 0.73 mmol) in Et$_2$O (20 mL). The colorless solution was stirred for 2 h, and the volatiles were pumped off to yield a sticky solid. Repeated washing with dicholoromethane and pentane followed by drying in vacuo afforded **17** as a colorless powder. Yield 0.88 g (78%). Crystals of the ethanol adduct **{{17}$_4$·EtOH}·3CH$_2$Cl$_2$** were isolated from a CH$_2$Cl$_2$/pentane mixture stored at room temperature. $^1$H NMR (CD$_2$Cl$_2$, 500.13 MHz, 298 K): $\delta$ 5.71 (br, 2H, N*H*$_2$), 3.94−3.77 (m, 16H, O-C*H*$_2$), 2.95 (s, 2H, C*H*$_2$-C(CF$_3$)$_2$O), 2.90−2.82 (m, 4H, N-C*H*$_2$-CH$_2$-O) ppm. $^{13}$C{$^1$H} NMR (CD$_2$Cl$_2$, 125.76 MHz, 298 K): $\delta$ 149.3, 147.4, 140.5, 138.6, 138.2, 136.2 (all $C_6F_5$), 126.8 (q, $^1J_{CF}$ = 290, *C*F$_3$), 80.4 (hept, $^2J_{CF}$ = 26, *C*(CF$_3$)$_2$), 70.0, 69.0, 68.9, 68.8 (all O-*C*H$_2$-*C*H$_2$-O), 56.0 (CH$_2$-*C*(CF$_3$)$_2$O), 55.8 (N-*C*H$_2$-CH$_2$) ppm.


dx.doi.org/10.1021/ja2024977 |J. Am. Chem. Soc. 2011, 133, 9069–9087

$^{19}F\{^{1}H\}$ NMR ($CD_2Cl_2$, 188.29 MHz, 298 K): $\delta$ −78.0 (s, 6F, $C(CF_3)_2$), −133.4 (d, $^3J_{FF}$ = 18.9, 12F, *o*-F), −160.6 (t, $^3J_{FF}$ = 18.9, 6F, *p*-F), −166.1 (d, $^3J_{FF}$ = 18.9, 12F, *m*-F) ppm. $^{11}B$ NMR (96.29 MHz, $CD_2Cl_2$, 298 K): $\delta$ −8.4 ppm. Anal. Calcd for $C_{50}H_{24}B_2BaF_{36}N_2O_5$ (1575.64 g·mol$^{-1}$): C 38.1, H 1.5, N 1.8. Found: C 38.3, H 1.8, N 1.7.

**Typical Polymerization Procedure.** In a glovebox, the metallic catalyst was placed in a Schlenk flask, while the monomer was loaded in a bent glass finger. The Schlenk flask and bent finger were sealed and removed from the glovebox. All subsequent operations were carried out on a vacuum line using Schlenk techniques. The required amount of solvent was added with a syringe to the Schlenk flask containing the catalyst. The initiator ($^i$PrOH or BnOH) was then added, and the resulting mixture was stirred at the desired temperature until complete dissolution of the solids was ensured. The monomer was added with the bent finger, and the polymerization time was measured from this point. The reaction was terminated by addition of acidified MeOH (HCl, 10 wt-%) and the polymer was precipitated in methanol and washed thoroughly. The polymer was then dried to constant weight in a vacuum oven at 55 °C under dynamic vacuum (<5·10$^{-2}$ mbar).

**NMR Kinetics Measurements.** In a typical experiment, the catalyst and monomer were loaded in an NMR tube in a glovebox. The NMR tube was placed in a Schlenk tube, which was then removed from the glovebox and connected to the Schlenk manifold. All subsequent operations were performed using Schlenk techniques. The appropriate amounts of solvent (toluene-$d_8$) and initiator (BnOH or *i*PrOH) were added to the NMR tube in this order at room temperature,[68] and the NMR tube was then sealed and introduced in the spectrometer preset at the desired temperature. Kinetic measurements started from this point. Data points were collected at regular intervals (typically 45−70 s, with D1 = 0.5 s and NS = 4 or 8 scans) until conversion of the monomer stopped (this usually coincided with full conversion). The conversion was reliably determined by integrating the methine region of PLLA ($\delta$ 5.05 ppm at 100 °C in toluene-$d_8$) versus that of the monomer ($\delta$ 4.34 ppm at 100 °C in toluene-$d_8$). The accuracy of the measurements was corroborated by the good agreement between theoretical (based on the conversion, $M_{n,theo}$ = 144.13 × [L-LA]$_0$/[ROH]$_0$ × conversion) and experimental ($M_{n,NMR}$ determined by integration of the resonance of the methine protons vs that of the chain-ends) molecular weights.

**X-ray Crystallography.** Diffraction data were collected using a Bruker APEX CCD diffractometer with graphite-monochromated Mo K$\alpha$ radiation ($\lambda$ = 0.71073 Å). A combination of $\omega$ and $\Phi$ scans was carried out to obtain at least a unique data set. The crystal structures were solved by direct methods, and remaining atoms were located from difference Fourier synthesis followed by full-matrix least-squares refinement based on F2 (programs SIR97 and SHELXL-97).[69] Crystal data and details of data collection and structure refinement for all compounds (CCDC 816019−816026 and 816563) can be obtained free of charge from the Cambridge Crystallographic Data Centre via www.ccdc.cam.ac.uk/data_request/cif.

**Computational Details.** Calculations were carried out at the DFT level using the hybrid functional B3PW91[70] with the Gaussian 03[71] suite of programs. Barium, strontium, and silicon were treated with a relativistic effective-core potential (RECP)[72] from the Stuttgart group and the corresponding optimized basis set. Polarized all-electron double-$\zeta$ 6-31G(d,p)[73] basis sets were used for C, H, O, and N, a triple-$\zeta$ 6-311G augmented by a polarization and a diffuse function was used for Ca atoms.[74] Geometry optimizations were carried out without any symmetry restriction. The nature of the extrema (minimum or transition state) was verified with analytical frequency calculations. NBO analysis was carried out on all complexes.[75]

## ■ ASSOCIATED CONTENT

**Supporting Information.** Details of the general experimental and analytical procedures; solid-state structures of compounds **1**, **3**·$CH_2Cl_2$, **7**, and **8**; crystallographic data for **1**, **3**·$CH_2Cl_2$, **7**, **8**, and **13**-{{**17**}$_4$·**EtOH**}·3$CH_2Cl_2$ as CIF files; tables of crystallographic data; full polymerization data; $^1$H NMR and MALDI-TOF mass spectrometry analyses of PLLA samples prepared with **8**−**17** and $^i$PrOH or BnOH; plots for the kinetic studies of the polymerization of L-LA promoted by **13**−**17**/BnOH; NMR data for the reaction [L-LA]$_0$/[**16**]$_0$/[BnOH]$_0$ = 10:1:10 in $CD_2Cl_2$; Cartesian coordinates of DFT-optimized structures; complete ref 71. This material is available free of charge via the Internet at http://pubs.acs.org.

## ■ AUTHOR INFORMATION

**Corresponding Authors**

yann.sarazin@univ-rennes1.fr; jean-francois.carpentier@univ-rennes1.fr

## ■ ACKNOWLEDGMENT

The authors are very grateful to CNRS and the *Institut Universitaire de France* (J.-F.C., L.M.) for their financial support. We also thank Stephen Boyer (London Metropolitan University) for carrying out all elemental analyses and Total Petrochemicals for the generous gift of L-lactide.

## ■ REFERENCES

(1) (a) Uhrich, K. E; Cannizzaro, S. M.; Langer, R. S.; Shakesheff, K. M. *Chem. Rev.* **1999**, *99*, 3181–3198. (b) Drumright, R. E.; Gruber, P. R.; Henton, D. E. *Adv. Mater.* **2000**, *12*, 1841–1846. (c) Albertsson, A.-C.; Varma, I. K. *Biomacromolecules* **2003**, *4*, 1466–1486. (d) Mecking, S. *Angew. Chem., Int. Ed.* **2004**, *43*, 1078–1085. (e) Dechy-Cabaret, O.; Martin-Vaca, B.; Bourissou, D. *Chem. Rev.* **2004**, *104*, 6147–6176.

(2) (a) Ragauskas, A. J.; Williams, C. K.; Davison, B. H.; Britovsek, G.; Cairney, J.; Eckert, C. A.; Frederick, W. J., Jr.; Hallett, J. P.; Leak, D. J.; Liotta, C. L.; Mielenz, J. R.; Murphy, R.; Templer, R.; Tschaplinski, T. *Science* **2006**, *311*, 484–489. (b) Bozell, J. J.; Petersen, G. R. *Green Chem.* **2010**, *12*, 539–554.

(3) *Biopolymers from Renewable Resources*; Kaplan, D. L., Ed.; Springer: Berlin, 1998.

(4) Okada, M. *Prog. Polym. Sci.* **2002**, *27*, 87–133.

(5) (a) McLain, S. J.; Ford, T. M.; Drysdale, N. E. *Polym. Prepr. (Am. Chem. Soc., Div. Polym. Chem.)* **1992**, *33*, 463–464. (b) Ovitt, T. M.; Coates, G. W. *J. Am. Chem. Soc.* **1999**, *121*, 4072–4073. (c) Cai, C.-X.; Amgoune, A.; Lehmann, C. W.; Carpentier, J.-F. *Chem. Commun.* **2004**, 330–331. (d) Amgoune, A.; Thomas, C. M.; Roisnel, T.; Carpentier, J.-F. *Chem.—Eur. J.* **2006**, *12*, 169–179. (e) Amgoune, A.; Thomas, C. M.; Carpentier, J.-F. *Pure Appl. Chem.* **2007**, *79*, 2013–2030. (f) Dyer, H. E.; Huijser, S.; Schwarz, A. D.; Wang, C.; Duchateau, R.; Mountford, P. *Dalton Trans.* **2008**, 32–35. (g) Ajellal, N.; Lyubov, D. M.; Sinenkov, M. A.; Fukin, G. K.; Cherkasov, A. V.; Thomas, C. M.; Carpentier, J.-F.; Trifonov, A. A. *Chem.—Eur. J.* **2008**, *14*, 5440–5448. (h) Otero, A.; Fernández-Baeza, J.; Lara-Sánchez, A.; Alonso-Moreno, C.; Márquez-Segovia, I.; Sánchez-Barba, L. F.; Rodríguez, A. M. *Angew. Chem., Int. Ed.* **2009**, *48*, 2176–2179. (i) Kramer, J. W.; Treitler, D. S.; Dunn, E. W.; Castro, P. M.; Roisnel, T.; Thomas, C. M.; Coates, G. W. *J. Am. Chem. Soc.* **2009**, *131*, 16042–16044. (j) Mahrova, T. V.; Fukin, G. K.; Cherkasov, A. V.; Trifonov, A. A.; Ajellal, N.; Carpentier, J.-F. *Inorg. Chem.* **2009**, *48*, 4258–4266. (k) Zhang, Z.; Xu, X.; Sun, S.; Yao, Y.; Zhang, Y.; Shen, Q. *Chem. Commun.* **2009**, 7414–7416. (l) Zhang, Z.; Xu, X.; Li, W.; Yao, Y.; Zhang, Y.; Shen, Q.; Luo, Y. *Inorg. Chem.* **2009**, *48*, 5715–5724. (m) Platel, R. H.; White, A. J. P.; Williams, C. K. *Chem. Commun.* **2009**, 4115–4117. (n) Clark, L.; Cushion, M. G.; Dyer, H. E.; Schwarz, A. D.; Duchateau, R.; Mountford, P. *Chem. Commun.* **2010**, *46*, 273–275. (o) Nie, K.; Gu, X.; Yao, Y.; Zhang, Y.; Shen, Q. *Dalton Trans.* **2010**, *39*, 6832–6840. (p) Luo, Y.; Li, W.; Lin, D.; Yao, Y.; Zhang,

Y.; Shen, Q. *Organometallics* **2010**, *29*, 3507–3514. (q) Dyer, H. E.; Huijser, S.; Susperregui, N.; Bonnet, F.; Schwarz, A. D.; Duchateau, R.; Maron, L.; Mountford, P. *Organometallics* **2010**, *29*, 3602–3621. (r) Grunova, E.; Kirillov, E.; Roisnel, T.; Carpentier, J.-F. *Dalton Trans.* **2010**, *39*, 6739–6752. (s) Bouyahyi, M.; Ajellal, N.; Kirillov, E.; Thomas, C. M.; Carpentier, J.-F. *Chem.—Eur. J.* **2011**, *17*, 1872–1883.

(6) (a) Le Borgne, A.; Vincens, V.; Jouglard, M.; Spassky, N. *Makromol. Chem., Macromol. Symp.* **1993**, *73*, 37–46. (b) Wisniewski, M.; Le Borgne, A.; Spassky, N. *Macromol. Chem. Phys.* **1997**, *198*, 1227–1238. (c) Ovitt, T. M.; Coates, G. W. *J. Am. Chem. Soc.* **2002**, *124*, 1316–1326. (d) Nomura, N.; Ishii, R.; Akakura, M.; Aoi, K. *J. Am. Chem. Soc.* **2002**, *124*, 5938–5939. (e) Nomura, N.; Ishii, R.; Yamamoto, Y.; Kondo, T. *Chem.—Eur. J.* **2007**, *13*, 4433–4451. (f) Bouyahyi, M.; Grunova, E.; Marquet, N.; Kirillov, E.; Thomas, C. M.; Roisnel, T.; Carpentier, J.-F. *Organometallics* **2008**, *27*, 5815–5825. (g) Du, H.; Velders, A. H.; Dijkstra, P. J.; Zhong, Z.; Chen, X.; Feijen, J. *Macromolecules* **2009**, *42*, 1058–1066. (h) Du, H.; Velders, A. H.; Dijkstra, P. J.; Sun, J.; Zhong, Z.; Chen, X.; Feijen, J. *Chem.—Eur. J.* **2009**, *15*, 9836–9845. (i) Nomura, N.; Akita, A.; Ishii, R.; Mizuno, M. *J. Am. Chem. Soc.* **2010**, *132*, 1750–1751. (j) Schwarz, A. D.; Chu, Z.; Mountford, P. *Organometallics* **2010**, *29*, 1246–1260. (k) Bouyahyi, M.; Roisnel, T.; Carpentier, J.-F. *Organometallics* **2010**, *29*, 491–500. (l) Otero, A.; Lara-Sánchez, A.; Fernández-Baeza, J.; Alonso-Moreno, C.; Castro-Osma, J. A.; Márquez-Segovia, I.; Sánchez-Barba, L. F.; Rodríguez, A. M.; Garcia-Martinez, J. C. *Organometallics* **2011**, *30*, 1507–1522.

(7) Indium ROP initiators have been also described very recently: (a) Douglas, A. F.; Patrick, B. O.; Mehrkhodavandi, P. *Angew. Chem., Int. Ed.* **2008**, *47*, 2290–2293. (b) Peckermann, I.; Kapelski, A.; Spaniol, T. P.; Okuda, J. *Inorg. Chem.* **2009**, *48*, 5526–5534. (c) Pietrangelo, A.; Hillmyer, M. A.; Tolman, W. B. *Chem. Commun.* **2009**, 2736–2737. (d) Pietrangelo, A.; Knight, S. C.; Gupta, A. K.; Yao, L. J.; Hillmyer, M. A.; Tolman, W. B. J. *Am. Chem. Soc.* **2010**, *132*, 11649–11657. (e) Buffet, J.-C.; Okuda, J.; Arnold, P. L. *Inorg. Chem.* **2010**, *49*, 419–426. (f) Blake, M. P.; Schwarz, A. D.; Mountford, P. *Organometallics* **2011**, *30*, 1202–1214.

(8) (a) Cheng, M.; Attygalle, A. B.; Lobkovsky, E. B.; Coates, G. W. *J. Am. Chem. Soc.* **1999**, *121*, 11583–11584. (b) Chamberlain, B. M.; Cheng, M.; Moore, D. R.; Ovitt, T. M.; Lobkovsky, E. B.; Coates, G. W. *J. Am. Chem. Soc.* **2001**, *123*, 3229–3238. (c) Williams, C. K.; Breyfogle, L. E.; Choi, S. K.; Nam, W.; Young, V. G., Jr.; Hillmyer, M. A.; Tolman, W. B. *J. Am. Chem. Soc.* **2003**, *125*, 11350–11359. (d) Chen, C.-T.; Chan, C.-Y.; Huang, C.-A.; Chen, M.-T.; Peng, K.-F. *Dalton Trans.* **2007**, 4073–4078. (e) Silvernail, C. M.; Yao, L. J.; Hill, L. M. R.; Hillmyer, M. A.; Tolman, W. B. *Inorg. Chem.* **2007**, *46*, 6565–6574. (f) Alonso-Moreno, C.; Garcés, A.; Sánchez-Barba, L. F.; Fajardo, M.; Fernández-Baeza, J.; Otero, A.; Lara-Sánchez, A.; Antiñolo, A.; Broomfield, L.; López-Solera, M. I.; Rodríguez, A. M. *Organometallics* **2008**, *27*, 1310–1321. (g) Börner, J.; Flörke, U.; Huber, K.; Döring, A.; Kuckling, D.; Herres-Pawlis, S. *Chem.—Eur. J.* **2009**, *15*, 2362–2376. (h) Poirier, V.; Roisnel, T.; Carpentier, J.-F.; Sarazin, Y. *Dalton Trans.* **2009**, 9820–9827. (i) Drouin, F.; Oguadinma, P. O.; J. J. Whitehorne, T.; Prud'homme, R. E.; Schaper, F. *Organometallics* **2010**, *29*, 2139–2147. (j) Darensbourg, D. J.; Karroonnirun, O. *Inorg. Chem.* **2010**, *49*, 2360–2371. (k) Darensbourg, D. J.; Karroonnirun, O. *Macromolecules* **2010**, *43*, 8880–8886. (l) Wang, L.; Ma, H. *Dalton Trans.* **2010**, *39*, 7897–7910. (m) Liang, L.-C.; Lee, W.-Y.; Tsai, T.-L.; Hsua, Y.-L.; Lee, T.-Y. *Dalton Trans.* **2010**, *39*, 8748–8758. (n) Poirier, V.; Roisnel, T.; Carpentier, J.-F.; Sarazin, Y. *Dalton Trans.* **2011**, *40*, 523–534.

(9) (a) O'Keefe, B. J.; Hillmyer, M. A.; Tolman, W. B. *J. Chem. Soc., Dalton Trans.* **2001**, 2215–2224. (b) Wu, J.; Yu, T.-L.; Chen, C.-T.; Lin, C.-C. *Coord. Chem. Rev.* **2006**, *250*, 602–626. (c) Wheaton, C. A.; Hayes, P. G.; Ireland, B. J. *Dalton Trans.* **2009**, 4832–4846. (d) Thomas, C. M. *Chem. Soc. Rev.* **2010**, *39*, 165–173. (e) Stanford, M. J.; Dove, A. P. *Chem. Soc. Rev.* **2010**, *39*, 486–494. (f) Carpentier, J.-F. *Macromol. Rapid Commun.* **2010**, *31*, 1696–1705.

(10) (a) Hannant, M. D.; Schormann, M.; Bochmann, M. *J. Chem. Soc., Dalton Trans.* **2002**, 4071–4073. (b) Sarazin, Y.; Schormann, M.; Bochmann, M. *Organometallics* **2004**, *23*, 3296–3302. (c) Hannant, M. D.; Schormann, M.; Hughes, D. L.; Bochmann, M. *Inorg. Chim. Acta* **2005**, *358*, 1683–1691. (d) Wheaton, C. A.; Ireland, B. J.; Hayes, P. G. *Organometallics* **2009**, *28*, 1282–1285. (e) Wheaton, C. A.; Hayes, P. G. *Dalton Trans.* **2010**, *39*, 3861–3869. (f) Wheaton, C. A.; Hayes, P. G. *Chem. Commun.* **2010**, *46*, 8404–8406.

(11) Ireland, B. J.; Wheaton, C. A.; Hayes, P. G. *Organometallics* **2010**, *29*, 1079–1084.

(12) (a) Sheng, H.-T; Zhou, H.; Guo, H.-D.; Sun, H.-M.; Yao, Y.-M.; Wang, J.-F.; Zhang, Y.; Shen, Q. *J. Organomet. Chem.* **2007**, *692*, 1118–1124. (b) Robert, D.; Kondracka, M.; Okuda, J. *Dalton Trans.* **2008**, 2667–2669. (c) Robert, D.; Abinet, E.; Spaniol, T. P.; Okuda, J. *Chem.—Eur. J.* **2009**, *15*, 11937–11947.

(13) For discrete aluminum cationic ROP initiators, see ref 6l and: (a) Emig, N.; Nguyen, H.; Krautscheid, H.; Réau, R.; Cazeaux, J.-B.; Bertrand, G. *Organometallics* **1998**, *17*, 3599–3608. (b) Robson, D. A.; Rees, L. H.; Mountford, P.; Schröder, M. *Chem. Commun.* **2000**, 1269–1270. (c) Lewiński, J.; Horeglad, P.; Dranka, M.; Justyniak, I. *Inorg. Chem.* **2004**, *43*, 5789–5791. (d) Milione, S.; Grisi, F.; Centore, R.; Tuzi, A. *Organometallics* **2006**, *25*, 266–274. (e) Dagorne, S.; Le Bideau, F.; Welter, R.; Bellemin-Laponnaz, S.; Maisse-François, A. *Chem.—Eur. J.* **2007**, *13*, 3202–3217. (f) Issenhuth, J.-T.; Pluvinage, J.; Welter, R.; Bellemin-Laponnaz, S.; Dagorne, S. *Eur. J. Inorg. Chem.* **2009**, 4701–4709. (g) Haddad, M.; Laghzaoui, M.; Welter, R.; Dagorne, S. *Organometallics* **2009**, *28*, 4584–4592. (h) Lian, B.; Ma, H.; Spaniol, T. P.; Okuda, J. *Dalton Trans.* **2009**, 9033–9042.

(14) A cationic silver ROP initiator has been described: Samantaray, M. K.; Katiyar, V.; Roy, D.; Pang, K.; Nanavati, H.; Stephen, R.; Sunoj, R. B.; Ghosh, P. *Eur. J. Inorg. Chem.* **2006**, 2975–2984.

(15) For comprehensive reviews on organic ROP initiators, see: (a) Kamber, N. E.; Jeong, W.; Waymouth, R. M.; Pratt, R. C.; Lohmeijer, B. G. G.; Hedrick, J. L. *Chem. Rev.* **2007**, *107*, 5813–5840. (b) Bourissou, D.; Moebs-Sanchez, S.; Martín-Vaca, B. *C. R. Chim.* **2007**, *10*, 775–794. (c) Kiesewetter, M. K.; Ji Shin, E.; Hedrick, J. L.; Waymouth, R. M. *Macromolecules* **2010**, *43*, 2093–2107.

(16) (a) Martin, E.; Dubois, P.; Jérôme, R. *Macromolecules* **2000**, *33*, 1530–1535. (b) Liu, Y.-C.; Ko, B.-T.; Lin, C.-C. *Macromolecules* **2001**, *34*, 6196–6201. (c) Hsueh, M.-L.; Huang, B.-H.; Lin, C.-C. *Macromolecules* **2002**, *35*, 5763–5768. (d) Amgoune, A.; Thomas, C. M.; Carpentier, J.-F. *Macromol. Rapid Commun.* **2007**, *28*, 693–697. (e) Helou, M.; Miserque, O.; Brusson, J.-M.; Carpentier, J.-F.; Guillaume, S. M. *Chem.—Eur. J.* **2008**, *14*, 8772–8775. (f) Guillaume, C.; Carpentier, J.-F.; Guillaume, S. M. *Polymer* **2009**, *50*, 5909–5917. (g) Poirier, V.; Duc, M.; Carpentier, J.-F.; Sarazin, Y. *ChemSusChem* **2010**, *3*, 579–590. (h) Ajellal, N.; Carpentier, J.-F.; Guillaume, C.; Guillaume, S. M.; Helou, M.; Poirier, V.; Sarazin, Y.; Trifonov, A. *Dalton Trans.* **2010**, *39*, 8363–8376. (i) Zhao, W.; Cui, D.; Liu, X.; Chen, X. *Macromolecules* **2010**, *43*, 6678–6684.

(17) (a) Asano, S.; Aida, T.; Inoue, S. J. *Chem. Soc., Chem. Commun.* **1985**, 1148–1149. (b) Aida, T.; Maekawa, Y.; Asano, S.; Inoue, S. *Macromolecules* **1988**, *21*, 1195–1202. (c) Sugimoto, H.; Aida, T.; Inoue, S. *Macromolecules* **1990**, *23*, 2869–2875. (d) Aida, T.; Inoue, S. *Acc. Chem. Res.* **1996**, *29*, 39–48. (e) Inoue, S. *J. Polym. Sci., Part A: Polym. Chem.* **2000**, *38*, 2861–2871.

(18) (a) Westerhausen, M.; Schneiderbauer, S.; Kneifel, A. N.; Söltl, Y.; Mayer, P.; Nöth, H.; Zhong, Z.; Dijkstra, P. J.; Feijen, J. *Eur. J. Inorg. Chem.* **2003**, 3432–3439. (b) Hill, M. S.; Hitchcock, P. B. *Chem. Commun.* **2003**, 1758–1759. (c) Chisholm, M. H.; Gallucci, J.; Phomphrai, K. *Chem. Commun.* **2003**, 48–49. (d) Chisholm, M. H.; Gallucci, J.; Phomphrai, K. *Inorg. Chem.* **2004**, *43*, 6717–6725. (e) Darensbourg, D. J.; Choi, W.; Richers, C. P. *Macromolecules* **2007**, *40*, 3521–3523. (f) Darensbourg, D. J.; Choi, W.; Karroonnirun, O.; Bhuvanesh, N. *Macromolecules* **2008**, *41*, 3493–3502. (g) Xu, X.; Chen, Y.; Zou, G.; Mac, Z.; Li, G. *J. Organomet. Chem.* **2010**, *695*, 1155–1162. (h) Sarazin, Y.; Roşca, D.; Poirier, V.; Roisnel, T.; Silvestru, A.; Maron, L.; Carpentier, J.-F. *Organometallics* **2010**, *29*, 6569–6577.

(19) For examples of molecular Ae initiators for ROP, see: (a) Zhong, Z.; Dijkstra, P. J.; Birg, C.; Westerhausen, M.; Feijen, J.

*Macromolecules* **2001**, *34*, 3863–3868. (b) Darensbourg, D. J.; Choi, W.; Ganguly, P.; Richers, C. P. *Macromolecules* **2006**, *39*, 4374–4379. (c) Sarazin, Y.; Howard, R. H.; Hughes, D. L.; Humphrey, S. M.; Bochmann, M. *Dalton Trans.* **2006**, 340–350. (d) Davidson, M. G.; O'Hara, C. T.; Jones, M. D.; Keir, C. G.; Mahon, M. F.; Kociok-Köhn, G. *Inorg. Chem.* **2007**, *46*, 7686–7688.

(20) Ionic radii for C.N. = 6: $Ca^{2+}$, 1.14; $Sr^{2+}$, 1.32; $Ba^{2+}$, 1.49 Å; see: Shannon, R. D. *Acta Crystallogr.* **1976**, *A32*, 751–767.

(21) (a) Hanusa, T. P. *Chem. Rev.* **1993**, *93*, 1023–1036. (b) Hanusa, T. P. *Coord. Chem. Rev.* **2000**, *210*, 329–367. (c) Alexander, J. S.; Ruhlandt-Senge, K. *Eur. J. Inorg. Chem.* **2002**, 2761–2774. (d) Buchanan, W. D.; Allis, D. G.; Ruhlandt-Senge, K. *Chem. Commun.* **2010**, *46*, 4449–4465.

(22) Chisholm, M. H. *Inorg. Chim. Acta* **2009**, *362*, 4284–4290 and references therein.

(23) (a) Crimmin, M. R.; Casely, I. J.; Hill, M. S. *J. Am. Chem. Soc.* **2005**, *127*, 2042–2043. (b) Harder, S.; Brettar, J. *Angew. Chem., Int. Ed.* **2006**, *45*, 3474–3478. (c) Crimmin, M. R.; Arrowsmith, M.; Barrett, A. G. M.; Casely, I. J.; Hill, M. S.; Procopiou, P. A. *J. Am. Chem. Soc.* **2009**, *131*, 9670–9685. (d) Sarish, S. P.; Nembenna, S.; Nagendran, S.; Roesky, H. W. *Acc. Chem. Res.* **2011**, *44*, 157–170 and references therein.

(24) (a) Datta, S.; Roesky, P. W.; Blechert, S. *Organometallics* **2007**, *26*, 4392–4394. (b) Datta, S.; Gamer, M. T.; Roesky, P. W. *Organometallics* **2008**, *27*, 1207–1213.

(25) For other, less common ligands, see: (a) Arrowsmith, M.; Hill, M. S.; Kociok-Köhn, G. *Organometallics* **2009**, *28*, 1730–1738. (b) Arrowsmith, M.; Heath, A.; Hill, M. S.; Hitchcock, P. B.; Kociok-Köhn, G. *Organometallics* **2009**, *28*, 4550–4559. (c) Jenter, J.; Köppe, R.; Roesky, P. W. *Organometallics* **2011**, *30*, 1404–1413.

(26) Arrowsmith, M.; Hill, M. S.; Kociok-Köhn, G. *Organometallics* **2011**, *30*, 1291–1294.

(27) For organometallic precursors, see in particular: (a) Eaborn, C.; Hawkes, S. A.; Hitchcock, P. B.; Smith, J. D. *Chem. Commun.* **1997**, 1961–1962. (b) Harvey, M. J.; Hanusa, T. P.; Young, V. G., Jr. *Angew. Chem., Int. Ed.* **1999**, *38*, 217–219. (c) Crimmin, M. R.; Barrett, A. G. M.; Hill, M. S.; MacDougall, D. J.; Mahon, M. F.; Procopiou, P. A. *Chem.—Eur. J.* **2008**, *14*, 11292–11295. (d) Johns, A. M.; Chmely, S. C.; Hanusa, T. P. *Inorg. Chem.* **2009**, *48*, 1380–1384. (e) Jochmann, P.; Dols, T. S.; Spaniol, T. P.; Perrin, L.; Maron, L.; Okuda, J. *Angew. Chem., Int. Ed.* **2009**, *48*, 5715–5719. (f) Yan, K.; Upton, B. M.; Ellern, A.; Sadow, A. D. *J. Am. Chem. Soc.* **2009**, *131*, 15110–15111.

(28) For Ae-amide precursors, see refs 18h and 21d and also: (a) Gillett-Kunnath, M. M.; MacLellan, J. G.; Forsyth, C. M.; Andrews, P. C.; Deacon, G. B.; Ruhlandt-Senge, K. *Chem. Commun.* **2008**, 4490–4492. (b) Gärtner, M.; Görls, H.; Westerhausen, M. *Dalton Trans.* **2008**, 1574–1582. (c) Glock, C.; Görls, H.; Westerhausen, M. *Inorg. Chem.* **2009**, *48*, 394–399.

(29) For recent reviews on the catalytic activity of Ae complexes, see: (a) Westerhausen, M. *Z. Anorg. Allg. Chem.* **2009**, *635*, 13–32. (b) Barrett, A. G. M.; Crimmin, M. R.; Hill, M. S.; Procopiou, P. A. *Proc. R. Soc. A* **2010**, *466*, 927–963. (c) Harder, S. *Chem. Rev.* **2010**, *110*, 3852–3876. (d) Kobayashi, S.; Yamashita, Y. *Acc. Chem. Res.* **2011**, *44*, 58–71.

(30) For reviews, see: (a) Jordan, R. F. *Adv. Organomet. Chem.* **1991**, *32*, 325–387. (b) Chen, E. Y.-X; Marks, T. J. *Chem. Rev.* **2000**, *100*, 1391–1434. (c) Bochmann, M. *J. Organomet. Chem.* **2004**, *689*, 3982–3998. (d) Bochmann, M. *Organometallics* **2010**, *29*, 4711–4740.

(31) With related Zn complexes, the higher catalytic activity of cationic compounds with respect to their neutral analogues has been observed for the hydroamination of alkenes: (a) Zulys, A.; Dochnahl, M.; Hollmann, D.; Löhnwitz, K.; Herrmann, J.-S.; Roesky, P. W.; Blechert, S. *Angew. Chem., Int. Ed.* **2005**, *44*, 7794–7798. (b) Dochnahl, M.; Pissarek, J.-W.; Blechert, S.; Löhnwitz, K; Roesky, P. W. *Chem. Commun.* **2006**, 3405–3407. (c) Dochnahl, M.; Löhnwitz, K.; Pissarek, J.-W.; Biyikal, M.; Schulz, S. R.; Schön, S.; Meyer, N.; Roesky, P. W.; Blechert, S. *Chem.—Eur. J.* **2007**, *13*, 6654–6666.

(32) Itoh, S.; Kumei, H.; Nagatomo, S.; Kitagawa, T.; Fukuzumi, S. *J. Am. Chem. Soc.* **2001**, *123*, 2165–2175.

(33) For a preliminary account, see: Sarazin, Y.; Poirier, V.; Roisnel, T.; Carpentier, J.-F. *Eur. J. Inorg. Chem.* **2010**, 3423–3428.

(34) Cushion, M. G.; Mountford, P. *Chem. Commun.* **2011**, *47*, 2276–2278.

(35) Fischer, R.; Langer, J.; Krieck, S.; Görls, H.; Westerhausen, M. *Organometallics* **2011**, *30*, 1359–1365.

(36) (a) Drake, S. R.; Otway, D. J.; Hursthouse, M. B.; Abdul Malik, K. M. *Polyhedron* **1992**, *11*, 1995–2007. (b) Tesh, K. F.; Hanusa, T. P.; Huffman, J. C.; Huffman, C. J. *Inorg. Chem.* **1992**, *31*, 5572–5579. (c) Tesh, K. F.; Burkey, D. J.; Hanusa, T. P. *J. Am. Chem. Soc.* **1994**, *116*, 2409–2417. (d) Chi, Y.; Ranjan, S.; Chou, T.-Y.; Liu, C.-S.; Peng, S.-M.; Lee, G.-H. *J. Chem. Soc., Dalton Trans.* **2001**, 2462–2466.

(37) For the formation of aggregated and polymetallic alkoxide-Ae species, see for instance: (a) Caulton, K. G.; Chisholm, M. H.; Drake, S. R.; Folting, K. *J. Chem. Soc., Chem. Commun.* **1990**, 1349–1350. (b) Caulton, K. G.; Chisholm, M. H.; Drake, S. R.; Huffman, J. C. *J. Chem. Soc., Chem. Commun.* **1990**, 1498–1499. (c) Goel, S. C.; Matchett, M. A.; Chiang, M. Y.; Buhro, W. E. *J. Am. Chem. Soc.* **1991**, *113*, 1844–1845. (d) Caulton, K. G.; Chisholm, M. H.; Drake, S. R.; Folting, K; Huffman, J. C. *Inorg. Chem.* **1993**, *32*, 816–820.

(38) Alexander, J. S.; Ruhlandt-Senge, K. *Chem.—Eur. J.* **2004**, *10*, 1274–1280.

(39) Carpentier, J.-F. *Dalton Trans.* **2010**, *39*, 37–48 and references cited therein.

(40) (a) Lancaster, S. J.; Rodriguez, A.; Lara-Sanchez, A.; Hannant, M. D.; Walker, D. A.; Hughes, D. L.; Bochmann, M. *Organometallics* **2002**, *21*, 451–453. (b) Sarazin, Y.; Hughes, D. L.; Kaltsoyannis, N.; Wright, J. A.; Bochmann, M. *J. Am. Chem. Soc.* **2007**, *129*, 881–894. (c) Sarazin, Y.; Kaltsoyannis, N.; Wright, J. A.; Bochmann, M. *Organometallics* **2007**, *26*, 1811–1815.

(41) Hannant, M. H.; Wright, J. A.; Lancaster, S. J.; Hughes, D. L.; Horton, P. N.; Bochmann, M. *Dalton Trans.* **2006**, 2415–2426.

(42) Bochmann, M. *Coord. Chem. Rev.* **2009**, *253*, 2000–2014.

(43) Groysman, S.; Sergeeva, E.; Goldberg, I.; Kol, M. *Inorg. Chem.* **2005**, *44*, 8188–8190.

(44) We have recently reported a strategy for the synthesis of stable $\{L_nX\}AeN(SiMe_2H)_2$ heteroleptic complexes (Ae = Ca, Sr, Ba); see ref 18h. The implementation of this method for the preparation of a broad range of heteroleptic Ae complexes is beyond the scope of the present study and will be the object of a separate report.

(45) The syntheses and characterization of **8**—**12** were reported in a preliminary account[33] and will not be discussed further here.

(46) (a) Pauling, L. *The Nature of the Chemical Bond*; Cornell University Press: Ithaca, NY, 1960; p 260. (b) Bondi, A. *J. Phys. Chem.* **1964**, *68*, 441–451.

(47) (a) Bradley, D. C.; Hasan, M.; Hursthouse, M. B.; Khan, O. F. Z.; Pritchard, R. G.; Williams, J. D. *J. Chem. Soc., Chem. Commun.* **1992**, 575–576. (b) Plenio, H. *Chem. Rev.* **1997**, *97*, 3363–3384. (c) Barrett, A. G. M.; Crimmin, M. R.; Hill, M. S.; Hitchcock, P. B.; Procopiou, P. A. *Angew. Chem., Int. Ed.* **2007**, *46*, 6339–6342.

(48) Reger, D. L.; Little, C. A.; Smith, M. D.; Rheingold, A. L.; Liable-Sands, L. M.; Yap, G. P. A.; Guzei, I. A. *Inorg. Chem.* **2002**, *41*, 19–27.

(49) Drozdov, A.; Troyanov, S. *J. Chem. Soc., Chem. Commun.* **1993**, 1619–1621.

(50) For instance, the polymerization of L-LA with **6** and $[L\text{-}LA]_0/[\mathbf{6}]_0/[BnOH]_0 = 1\,000/1/10$ in toluene at 30 °C gave 94% conversion within 60 min, but only afforded moderate control: $M_{n,theo} = 13\,700$ g·mol$^{-1}$, $M_{n,SEC}$ (corrected) = 12 000 g·mol$^{-1}$, $M_w/M_n = 1.69$.

(51) Note that **8** also promotes the ROP of L-LA without addition of $^i$PrOH, but the polymerization is not controlled in this case: the molecular weight distribution is broad ($M_w/M_n = 1.70$), and the experimental molecular weight does not match its theoretical value. The polymerization in this case results either from a cationic mechanism, or from the presence of traces of protic impurities which act as initiator.

(52) Save, M.; Schappacher, M.; Soum, A. *Macromol. Chem. Phys.* **2002**, *203*, 889–899.

(53) For the determination of molecular weight of poly(trimethylene carbonate)s, various correcting factors are applied depending on the

expected molecular weights, see: Palard, I.; Schappacher, M.; Belloncle, B.; Soum, A.; Guillaume, S. M. *Chem.—Eur. J.* **2007**, *13*, 1511–1521.

(54) Under identical experimental conditions, the triflate salts Ca(OTf)$_2$ did not catalyse the polymerisation of L-LA.

(55) Chamberlain, B. M.; Jazdzewski, B. A.; Pink, M.; Hillmyer, M. A.; Tolman, W. B. *Macromolecules* **2000**, *33*, 3970–3977.

(56) The $k_{app}^{100,BnOH}$ value of 0.376 $h^{-1}$ found for **16**/BnOH compares favorably with that found under identical experimental conditions and temperature (100 °C) for **8**/$^i$PrOH (0.246 $h^{-1}$, see ref 33) but cannot be directly related to those determined here for **10**/BnOH and **10**/$^i$PrOH at 60 °C.

(57) Kowalski, A.; Libiszowski, J.; Duda, A.; Penczek, S. *Macromolecules* **2000**, *33*, 1964–1971.

(58) The following rate law was reported: $-d[LA]/dt = k_p \cdot [LA]\cdot[TEA]^{-0.352}$; see ref 16i.

(59) The limited temperature range was imposed by the boiling point of the solvent and the limited solubility of L-LA and PLLA in toluene at high concentration below 85 °C, which rendered the measurements inaccurate and non reproducible.

(60) Chisholm, M. H.; Delbridge, E. E. *New J. Chem.* **2003**, *27*, 1177–1183.

(61) The apparent rate constants $k_{app,8}^{55}$ = 0.00001, $k_{app,10}^{55}$ = 0.00007, $k_{app,11}^{25}$ = 0.00125 and $k_{app,12}^{25}$ = 0.00246 $s^{-1}$ were determined by $^1$H NMR for **8** (55 °C), **10** (55 °C), **11** (25 °C), and **12** (25 °C) ($[L\text{-}LA]_0$ = 2.0 M, $[L\text{-}LA]_0/[\mathbf{16}]_0/[ROH]_0$ = 360:1:3.6), respectively. However, the accuracy of the measurements was limited in these cases, as we found that polymerization was often initiated before the first point of analysis (especially with **11** and **12**) and that accurate determination of conversions was impeded by the poor solubilities of L-LA and especially PLLA at these temperatures. Owing to the high activity of complexes **10**—**12**, higher polymerization temperatures to obtain homogeneous reaction mixtures were not suited as clearly the mechanism was not controlled in this case.

(62) Gualco, P.; Mercy, M.; Ladeira, S.; Coppel, Y.; Maron, L.; Amgoune, A.; Bourissou, D. *Chem.—Eur. J.* **2010**, *16*, 10808–10817.

(63) Bercaw, J. E.; Durell, A. C.; Gray, H. B.; Green, J. C.; Hazari, N.; Labinger, J. A.; Winkler, J. R. *Inorg. Chem.* **2010**, *49*, 1801–1810.

(64) Lavanant, L.; Chou, T.-Y.; Chi, Y.; Lehmann, C. W.; Toupet, L.; Carpentier, J.-F. *Organometallics* **2004**, *23*, 5450–5458.

(65) Bochmann, M.; Bwembya, G.; Webb, K. J. *Inorg. Synth.* **1997**, *31*, 19–24.

(66) Westerhausen, M. *Inorg. Chem.* **1991**, *30*, 96–101.

(67) Boncella, J. M.; Coston, C. J.; Cammack, J. K. *Polyhedron* **1991**, *10*, 769–770.

(68) We have checked that with these systems, polymerization of L-LA does not occur under these conditions at room temperature except when complexes **8** or **9** are employed. In these two cases, polymerization prior to injection in the NMR probe can be inhibited by maintaining the NMR tube at low temperature.

(69) (a) Sheldrick, G. M. *SHELXS-97, Program for the Determination of Crystal Structures*; University of Goettingen: Germany, 1997. (b) Sheldrick, G. M. *SHELXL-97, Program for the Refinement of Crystal Structures*; University of Goettingen: Germany, 1997.

(70) (a) Perdew, J. P.; Wang, Y. *Phys. Rev. B.* **1992**, *45*, 13244–13249. (b) Becke, A. D. *J. Chem. Phys.* **1993**, *98*, 5648–5652.

(71) Frisch, M. J. et al. *Gaussian 03, Revision C.02*; Gaussian, Inc.:, Wallingford, CT, 2004.

(72) (a) Fuentealba, P.; von Szentpaly, L.; Preuss, H.; Stoll, H. *J. Phys. B* **1985**, *18*, 1287–1296. (b) Bergner, A.; Dolg, M.; Kuechle, W.; Stoll, H.; Preuss, H. *Mol. Phys.* **1993**, *80*, 1431–1441.

(73) Hariharan, P. C.; Pople, J. A. *Mol. Phys.* **1974**, *27*, 209–214.

(74) Blaudeau, J.-P.; McGrath, M. P.; Curtiss, L. A.; Radom, L. *J. Chem. Phys.* **1997**, *107*, 5016–5021.

(75) Reed, A. E.; Curtiss, L. A.; Weinhold, F. *Chem. Rev.* **1988**, *88*, 899–926.